

Eddy-enhanced primary production ~~accelerates bacterial growth~~ sustains heterotrophic microbial activities in the Eastern Tropical North Atlantic

Quentin Devresse¹, Kevin W. Becker¹, Arne Bendinger^{1,2}, Johannes Hahn^{1,3}, Anja Engel¹

¹GEOMARHelmholtz Centre for Ocean Research Kiel, Germany,

~~²Laboratoire~~²Laboratoire d'Etudes en Géophysique et Océanographie Spatiales (LEGOS), Université Toulouse, IRD, CNRS, CNES, UPS, Toulouse, France

~~³Bundesamt~~³Bundesamt für Seeschifffahrt und Hydrographie, Hamburg, Germany

Correspondence: Quentin Devresse (qdevresse@geomar.de)

Abstract

Mesoscale eddies ~~play essential roles in modulating~~modulate the ocean's physical, chemical, and biological properties. In cyclonic eddies (CE)), nutrient upwelling can stimulate primary production by phytoplankton. Yet, how this locally enhanced autotrophic production affects ~~heterotrophic bacterial activities (biomass production and respiration)~~heterotrophy and consequently the metabolic balance between the synthesis and the consumption of dissolved organic matter (DOM) remains largely unknown. To ~~address~~fill this gap, we investigated the horizontal and vertical variability of ~~phytoplankton~~auto- and heterotrophic ~~bacterial~~microbial activity (~~biomass production and respiration~~) within a CE that formed off Mauritania and along the ~900 km zonal corridor between ~~the coast of Mauretania~~Mauritania and the Cape Verde Islands in the eastern tropical North Atlantic (ETNA). ~~We additionally collected samples from a CE along this transect at high spatial resolution.~~Our results show ~~easeading effects of how the physical disturbances induced~~caused by ~~at~~the CE ~~on~~affected the biomass distribution of phyto- and bacterioplankton ~~biomass~~and ~~their~~ metabolic activities. ~~Specifically, the..~~ The injection of nutrients into the sunlit surface resulted in enhanced autotrophic ~~plankton~~pico- and ~~nanoplankton~~ abundance and ~~generally increased autotrophic~~ activity as indicated by Chlorophyll *a* (Chl-*a*) concentration, ~~DOM exudation, and~~primary ~~productivity~~production (PP) and ~~extracellular release rates~~. However, the detailed eddy survey ~~also~~ revealed an uneven distribution of these ~~parameters~~variables with, for example, the highest Chl-*a* concentrations and PP rates ~~occurring~~ near and just beyond the CE's periphery. The

heterotrophic bacterial activity was similarly variable. Optode-based community respiration (CR) bacterial respiration (BR) estimates and bacterial biomass production (BP) largely followed the trends of PP and Chl-*a*. Thus, a submesoscale spatial mosaic of heterotrophic bacterial abundance and activities occurred within the CE ~~studied here~~ that was closely related to variability in autotrophic production. ~~This was supported by~~ Consistent with this, we found a significant positive correlation between concentrations of semi-labile dissolved organic carbon (SL-DOC; here the sum of dissolved hydrolyzable amino acids and dissolved combined carbohydrates) and BR ~~measurements. Bacterial growth efficiency (BP/(BR+BP))estimates.~~ Extracellular release of carbon as indicated by primary production of dissolved organic carbon (PP_{DOC}) was variable (1.4-10.5%) within the CE with depth and carbon exudation was laterally and not always sufficient to compensate the bacterial carbon demand (~~BR+BP; 28.3-114.5%.~~ BCD: BR+BP) with PP_{DOC} accounting between 28% and 110% of the BCD. Bacterial growth efficiency (BGE: BP/BCD) ranged between 1.7 and 18.2%. We ~~have additionally~~ estimated the metabolic state ~~in our samples, which to~~ establish whether the CE was a source or a sink of organic carbon. We showed that the CE carried a strong autotrophic signal in the core ($PP/(BR+BP) > CR > 1$). ~~Overall, our~~ Our results ~~showsuggest~~ that submesoscale (0-10 km) processes lead to highly variable metabolic activities of both ~~phototrophie~~ photoautotrophic and heterotrophic ~~microbes, which has implications for biogeochemical models estimating oceanic carbon fluxes. Additionally, we~~ microorganisms. Overall, we revealed that the ~~CECEs~~ not only ~~trap~~ trap and ~~transport~~ transport coastal nutrients and organic carbon to the open ocean, but also ~~stimulates~~ stimulate phytoplankton growth generating freshly produced organic matter during westward propagation. This ~~organic matter may fuel~~ drives heterotrophic processes ~~in the open ocean~~ and may ~~help~~ contribute to ~~explain~~ the ~~often previously~~ observed net ~~heterotrophic metabolic state of these environments~~ heterotrophy in open Atlantic surface waters.

1. Introduction

Mesoscale eddies (10-100 km) are ubiquitous in the ocean affecting upper ocean biogeochemistry and ecology, ~~e.g.,~~ For example, upwelling of nutrients ~~influeneing inside~~ eddies can enhance primary production and carbon export (Cheney and Richardson, 1976; Arístegui et al., 1997). The sense of rotation and their vertical structure classifies cyclonic (CEs), anticyclonic (ACEs; e.g., Chelton et al., 2011) or anticyclonic mode water eddies

(ACMEs; D'Asaro 1988). In Eastern Boundary Upwelling Systems (EBUS), eddies ~~may typically~~ form by flow separation ~~of~~ along slope boundary currents at topographic headlands (D'Asaro, 1988; Molemaker et al., 2015; Thomsen et al., 2016). Eddies have lifespans from days to months and can travel several hundred to thousands of kilometers across ocean basins (Chelton et al., 2011). ~~They are complex dynamical regimes for organic matter and nutrient transport (Gruber et al., 2011).~~ In the North Atlantic Ocean, eddies generated in the highly productive Canary Upwelling System (CanUS) may laterally propagate to the oligotrophic Subtropical North Atlantic Gyre (SNAG), transporting ~~thereby~~ nutrients and carbon from the coast to the open ocean (McGillicuddy et al., 2003; Karstensen et al., 2015; Schütte et al., 2016). ~~A variety of~~ Various studies demonstrated the impact of eddies on primary production (PP) on a global scale. ~~Yet~~ However, the ~~magnitude effects~~ of ~~the eddy-induced flux eddies vary regionally,~~ and ~~its utilization depend on the model, the area investigated, and the degree of studies with higher spatial resolution and is of eddies combined with advances in in situ observation, remote sensing and modelling are~~ still ~~controversial (See needed to better describe the physical and biological properties of the upper ocean. (see review by~~ McGillicuddy, 2016 and references therein). For example, Couespel et al., (2021) performed global warming simulations using a representation of mid-latitude double-gyre circulation ~~and~~. They showed that at the finest model resolution ($1/27^\circ$), eddies can mitigate the decline of primary production ($\approx -12\%$ at $1/27^\circ$ vs. $\approx -26\%$ at 1°). Modeling studies have long urged consideration of the effects of eddies on PP at submesoscale levels (0.1-10 km) to provide more realistic estimates of the oceanic carbon cycle (Levy Lévy et al., 2001). ~~Thus, understanding the impact of mesoscale eddies on plankton productivity will help to better predict future carbon cycling in EBUS under global change scenarios.~~

Eddies modulate the mixed layer depth by upwelling (CEs), downwelling (ACEs), or frontogenesis from eddy-eddy interaction, thereby creating spatial variability of nutrient concentration within ~~and~~ around eddies on ~~length scales of 0.1-10 km~~ the submesoscale (see reviews by Mahadevan, 2016 and McGillicuddy, 2016). In addition, the nonlinear response of phytoplankton growth to nutrient availability and advection of phytoplankton by currents makes plankton distribution and community composition highly variable within and around eddies (Lochte and Pfannkuche 1987). As a consequence, the spatial distribution of PP across eddies can be highly variable (e.g., Falkowski et al., 1991; Ewart et al., 2008; Singh et al., 2015). ~~Still, insight into the distribution of phytoplankton and their activities within mesoscale eddies is~~

~~limited due to a lack of sufficient fine-scale vertical and horizontal resolution studies to adequately describe these distributions.~~

Bacterial activity is directly coupled to PP₂, as autotrophic cells release their main substrate dissolved organic matter (DOM), ~~the main substrate for heterotrophic bacteria and archaea (Thornton 2014).~~ DOM release ~~has been interpreted as a cellular overflow mechanism that expels by~~ phytoplankton mainly occurs via two mechanisms: 1) passive leakage of small molecules by diffusion across the cell membrane and 2) active exudation of DOM into the carbon produced in excess (Woods surrounding environment (Engel et al., 2004). Environmental conditions, such as temperature, nutrient availability (e.g., Borchard and Van Valen, 1990; Schartau et al., 2007). Therefore, Engel, 2012) and light conditions (e.g., Cherrier et al., 2015) affect the amount and the elemental stoichiometry of released DOM ~~compounds are often depleted in nutrients limiting autotrophic cell growth (Engel et al., 2002).~~ Patchiness of phytoplankton primary productivity and nutrient limitationavailability within eddies may thus lead to spatial heterogeneity of extracellular release rates (e.g., Lasternas et al., 2013; Rao et al., 2021) ~~with distinct and~~ DOM quality (e.g., Wear et al., 2020). DOM quality impacts bacterial biomass production (BP), bacterial respiration (BR), and, ~~thus the~~ bacterial growth efficiency (BGE; e.g., Neijssel and de Mattos, 1994; Russell and Cook, 1995); Robinson, 2008; Lipson, 2015). BGE is the ratio between BP and the bacterial carbon demand (BCD), which is the sum of ~~assimilated carbon that is~~ respired carbon and carbon ~~that is~~ incorporated into biomass (BP + BR). Lønborg et al., (2011) ~~established~~observed that BGE decreases with increasing C/N ratio of ~~the bioavailable DOM produced by~~ phytoplankton-derived DOM. BGE is a critical parameter for estimating the amount of consumed organic carbon ~~that is~~ used to build biomass by heterotrophic bacteria (Anderson and Ducklow 2001). So far, BGE ~~within eddies~~ has been reported for ACEs from the Mediterranean Sea (Christaki et al., ~~2011~~;2021) but not for CEs and ~~Mode Water Eddies~~ACMEs. In general, several studies showed a patchy distribution of bacterial abundance, BP (Ewart et al., 2008; Baltar et al., 2010), BR, (Mouriño-Carballido, 2009; Jiao et al., 2014), community respiration (CR) (~~;~~ Mouriño-Carballido and McGillicuddy, 2006; Mouriño-Carballido, 2009), and of the metabolic balance between the production and consumption of organic matter (Maixandau et al., 2005; Ewart et al., 2008; Mouriño-Carballido and McGillicuddy, 2006; Mouriño-Carballido, 2009) within eddies.

Yet, ~~how eddies affect microbial plankton dynamics and carbon flow is largely unknown. So far, phyto- and bacterioplankton insights into the~~ distribution of phytoplankton and their activities ~~were either studied separately or at relatively low spatial~~within mesoscale eddies are

130 ~~limited due to insufficient fine-scale vertical and horizontal~~ resolution. ~~Data studies to~~
131 ~~adequately describe these distributions. Thus, data~~ on eddy-induced changes in primary
132 production, extracellular release and semi-labile DOM concentration, and the responses of
133 heterotrophic microbial metabolic activities are scarce. Understanding how eddies modulate
134 microbial activities will enhance our knowledge about the fate of ~~autotrophically fixed~~ organic
135 carbon and the overall CO₂ source/sink function in the ocean, ~~and particularly in particular~~
136 ~~EBUS-, where eddy generation is high (Pegliasco et al., 2015).~~

137 Here, we studied the impact of a CE on microbial carbon cycling along a 900 km zonal corridor
138 of the westward propagating eddies between the Cape Verde Islands and the
139 ~~Mauretania~~Mauritania Upwelling System (13-20 °N), a sub-region of the CanUS (13-33 °N,
140 Arístegui et al., 2009). About 146 ± 44 eddies with a lifetime of more than 7 days are
141 generated per year in this region (Schütte et al., 2016). Along this corridor, ~~we~~ a CE was
142 sampled at high spatial resolution to resolve the heterogeneity of microbial processes at the
143 submesoscale. We determined phytoplankton (~~<20 μm~~ 20 μm) cell abundance, primary
144 production, and extracellular release. ~~We and~~ linked those ~~parameters~~ measurements of
145 autotrophic activity to semi-labile DOM concentration and heterotrophic bacterial activity. Our
146 study ~~gives~~ provides new insights into 1) microbial carbon cycling and 2) factors controlling
147 microbial metabolic activities within and around CE formed in EBUS.

149 2. Materials and Methods

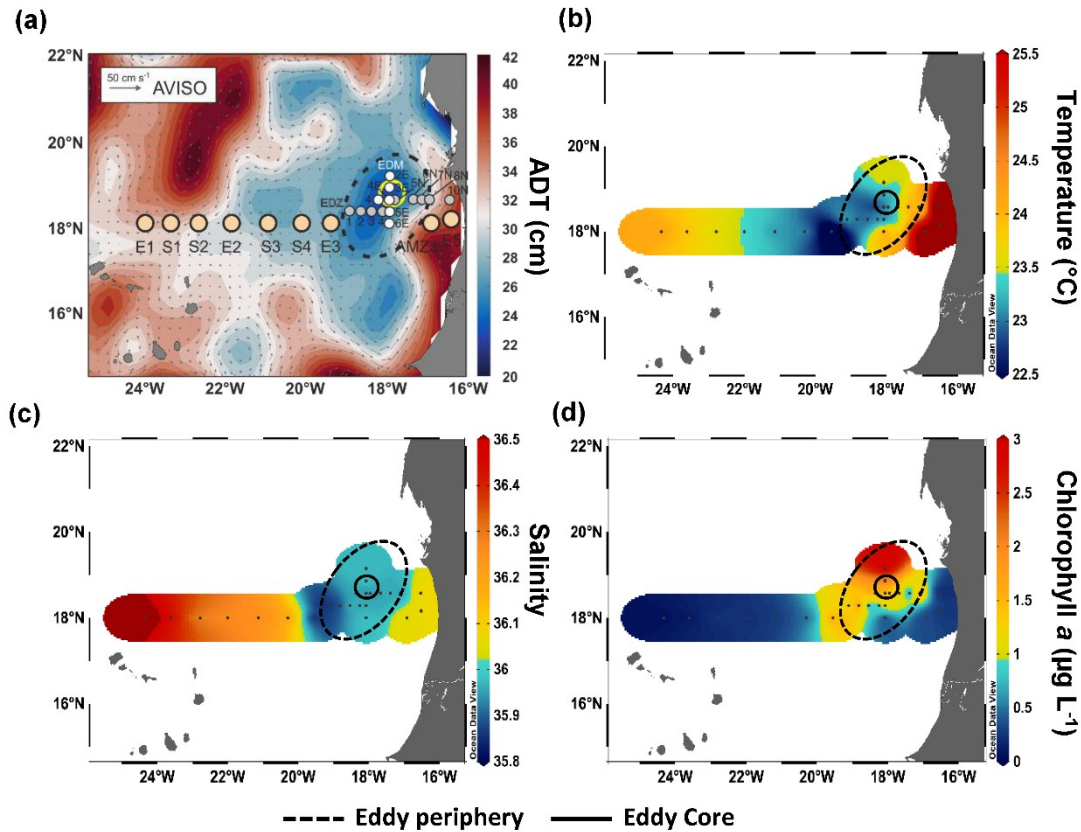
151 2.1 Study area and eddy characterization

153 Sampling was conducted in the ETNA between the Cape Verde archipelago and the
154 Mauritanian coast during cruise M156 (July 3rd to August 1st, 2019. Figure 1A) on the R/V
155 *Meteor*. Samples were collected during the relaxation period ~~(, which is typically~~ from May to
156 July) ~~that follows~~ following the upwelling season (January to March; Lathuilière et al., 2008).
157 A CE was sampled at high spatial resolution along two zonal transects (from 19.1 °W to 18.2
158 °W at 18.3 °N and from 18.5 °W to 17.1 °W at 18.6 °N) and one meridional ~~transects~~ transect
159 (from 19.4 °N to 18 °N at 18.4 °W to 18.1 °W). The zonal ~~section~~ was transect slightly
160 ~~meridionally~~ shifted east/west of the eddy core position. The reason for that was the deformed
161 eddy shape, (see Fig. 1A), which ~~resulted in a consecutive optimized identification~~ made it

~~challenging to identify the center~~ of the eddy ~~core position~~ and required rerouting of the ship's track during the eddy-survey. In addition, we sampled water along ~~the~~an 18 °N transect, a typical coast to open ocean trajectory of eddies in ~~the~~this region (Schütte et al., 2016). Salinity, temperature, depth, and O₂ concentration were determined ~~at each station~~ using a Seabird 911 plus CTD system equipped with two independently working sets of temperature-conductivity-oxygen sensors. The oxygen sensor was calibrated against discrete water samples using the Winkler method (Strickland and Parsons, 1968; Wilhelm, 1888). Seawater samples were collected ~~from the top 200 m~~ using ~~10 L~~10 L Niskin bottles attached to the CTD Rosette. A total of 25 stations ([SI Table S1](#)) were sampled; 14 of them inside or in the vicinity of the CE. Sampling was conducted in the epipelagic layer (0-200 m), including ~~water~~samples from the surface, ~~within the~~ mixed layer, ~~at the~~ Chl-*a* maximum, and ~~within~~ the shallow oxygen minimum zone (OMZ; <50 µmol kg⁻¹ between 0-200 m depth) when present.

Sea surface height (SSH) and Acoustic Doppler Current Profiler (ADCP) velocity data ([SI Fig. 1](#)) characterized the eddy as a CE. Based on the Angular Momentum Eddy Detection and Tracking Algorithm (AMEDA; Le Vu et al., 2018), the eddy was estimated to be 1.5 months old. The center of the eddy and the core radius were determined using ADCP ~~reconstruction~~reconstructions assuming an axis-symmetric vortex. ([SI Fig. 1](#)). On ~~22/07/July~~22nd 2019, the eddy center was located at 18.69 °N, 18.05 °W, with a core radius of 40.5 ± 5.7 km. The mean azimuthal velocity in the CE was 19.9 ± 0.7 cm s⁻¹ and the absolute dynamic topography associated with the CE core was ~23 cm on ~~23/07/19~~July 23rd 2019. Fine-scale analysis of the eddy physics will be given by Fischer et al. (2022, in prep). However, as the eddy shape was deformed, ADCP reconstruction did not constrain well the physical border of the eddy ([SI Fig. 1](#)–[S1](#)). Therefore, we combined sea surface temperature (23.44 ± 0.47 °C), salinity (39.95 ± 0.04) and Chl-*a* (1.35 ± 0.73 µg L⁻¹) data to approximate the area influenced by the eddy ([Fig. 1b,c,d](#)). We classified stations into ‘core’ and ‘periphery’ of the eddy. Stations that were outside and westward of the eddy influence were referred to as ‘open ocean’ and those close to the coast as ‘coastal’. ~~At~~Just beyond the ~~St. E3, outside of the CE~~eddy periphery, ~~we~~at ~~St. E3, a front was~~ observed ~~a front~~ with surface temperature and salinity (not ~~compensating~~ ~~incompensated by~~ density) ~~being clearly~~ different from ~~among~~ the adjacent stations ([Fig. 1b](#)), ~~potentially which might be related to enhanced, an up and downwelling might have occurred there on either side of the front, respectively.~~ Hence, we referred to that station as ‘Frontal Zone’. The classification of stations is thoroughly discussed in the supplementary information

(SI), and the sampling time, location, and distance from the eddy center are given in [SI Table S1](#).



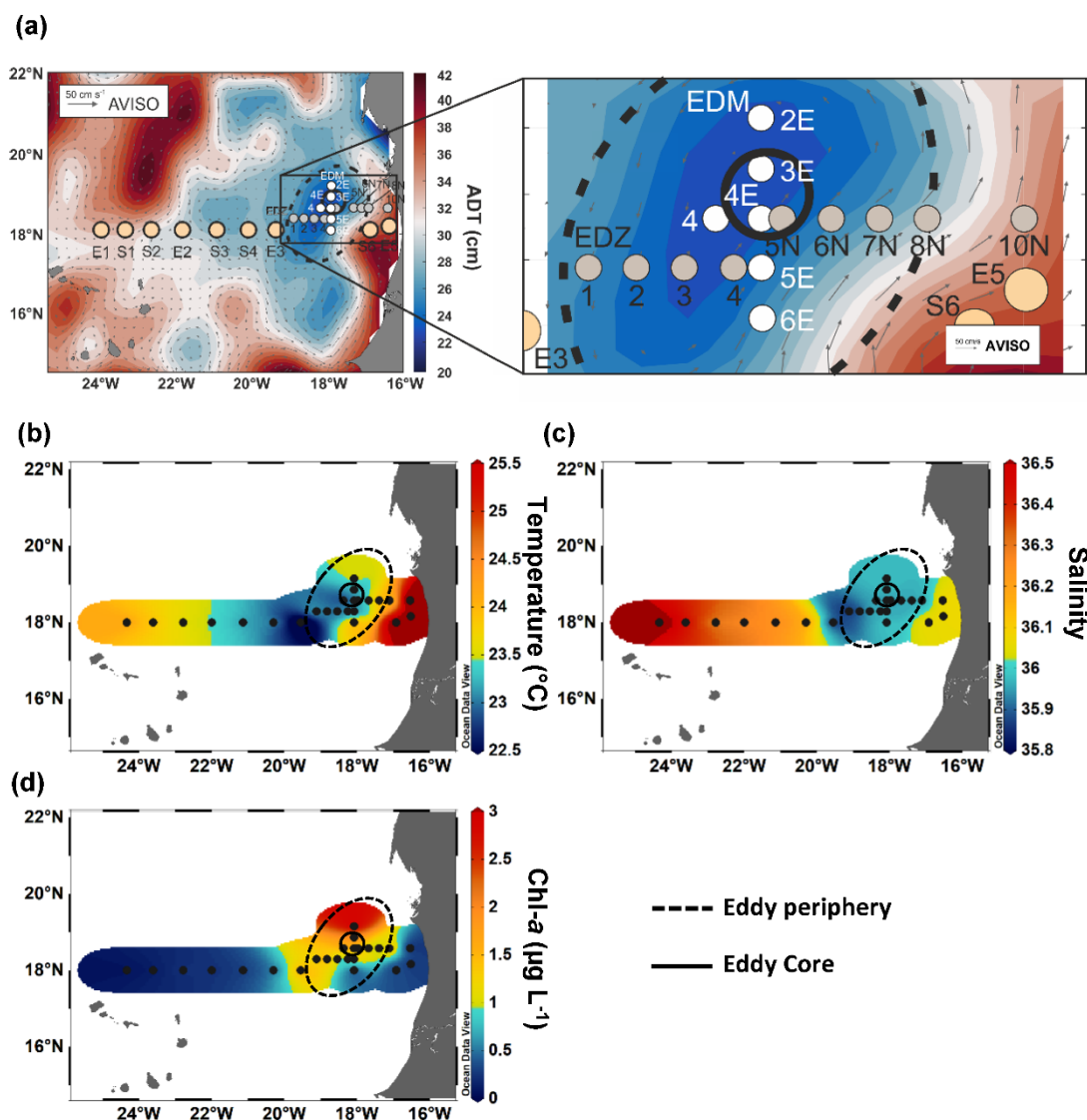


Figure 1: M156 Sampling stations during RV Meteor cruise track M156 including zoom in into the eddy
(a) Temperature, temperature at 5m depth (b) Salinity, salinity at 5m depth (c), and
chlorophyll a at 5m depth (d). The color background in (a) shows the variations in Absolute
Dynamic Topography (ADT) obtained from www.aviso.altimetry.fr. The direction and speed of
surface water geostrophic currents are shown as arrows. The solid circle in (a) – (d) indicates the core
of the eddy and the dashed circle outlines the periphery.

2.2 Chemical analyses

Nutrient concentrations were determined at selected stations (SI Table [4S1](#)). Nutrients were measured onboard from duplicate samples (11 mL) of unfiltered seawater samples (11 mL). Ammonium (NH_4^+) was analyzed after Solórzano (1969) and phosphate (PO_4), nitrate (NO_3^-),

nitrite (NO_2^-) and silicate ($\text{Si}(\text{OH})_4$) were measured photometrically with continuous-flow analysis on an auto-analyzer (QuAatro; Seal Analytical) after Grasshoff et al., (1999). Detection limits for NH_4^+ , PO_4 , NO_3 , NO_2 , and $\text{Si}(\text{OH})_4$ were 0.1, 0.02, 0.1, 0.02, and 0.2 $\mu\text{mol L}^{-1}$, respectively. ~~Total dissolved.~~ Dissolved inorganic nitrogen (DIN) was ~~determined~~ calculated as the sum of NH_4^+ , NO_3^- , and NO_2^- .

To estimate the fraction of semi-labile dissolved organic carbon (SL-DOC), we determined high-molecular-weight ($\text{HMW} > 1 \text{ kDa}$) dissolved combined carbohydrates (dCCHO) and dissolved hydrolysable amino acids (~~dAAdHAA~~) as the main biochemical components of DOM.

~~Duplicate~~ (Carlson, 2002). For dCCHO analysis, duplicate samples (20 mL) ~~for dCCHO~~ were filtered through 0.45 μm Acrodisc filters, collected in combusted glass vials (8 h, 450 °C) and frozen (-20°C) until analysis after Engel ~~&and~~ Händel (2011) with a detection limit of 1 $\mu\text{g L}^{-1}$. The analysis detected 11 monomers: arabinose, fucose, galactose, galactosamine, galacturonic acid, glucosamine, glucose, glucuronic acid, rhamnose, co-elute mannose, and xylose.

~~Duplicate~~ For dHAA analysis, duplicate samples (4 mL) ~~for dHAA~~ were filtered through ~~0.45 μm~~ 45 μm Acrodisc filters, collected in combusted glass vials (8 h, 450 °C), and frozen (-20°C) until analysis. ~~dAAdHAA~~ were measured with ortho-phthalaldehyde derivatization by high-performance liquid chromatography (HPLC; Agilent Technologies, USA) equipped with a C_{18} column (Phenomenex, USA) (Lindroth and Mopper, 1979; Dittmar et al., 2009). The analysis classified 13 monomers with a precision $< 5\%$ and a detection limit of 2 nmol L^{-1} : alanine, arginine, aspartic acid, isoleucine, glutamic acid, glycine, leucine, phenylalanine, serine, threonine, tyrosine, valine; and γ -aminobutyric acid (GABA).

The calculations for the carbon content of dCCHO and dHAA were based on carbon atoms contained in the identified monomers. The sum of dCCHO and dHAA carbon content is referred to as ~~semi-labile DOC~~ (SL-DOC).

For Chl-*a*, ~~1 L~~ seawater samples were ~~collected on~~ filtered onto 25 mm GF/F ~~(filters~~ (0.7 μm pore size, Whatman, GE Healthcare Life Sciences, UK) and subsequently frozen (-20°C) until extraction using 90-% acetone for photometric analyses (Turner Designs, USA) ~~),~~ slightly modified after Evans et al., (1987).

Bacteria were quantified using a flow cytometer (FACSCalibur, Becton Dickinson, Oxford, UK). Seawater samples (1.7 mL) were fixed with 85 μ L glutaraldehyde (1% final concentration) and stored at -80 °C until ~~enumeration~~analysis. Samples were stained with SYBR Green I (molecular probes) and ~~were~~ enumerated with a laser emitting at 488 nm and detected by their signature in a plot of side scatter (SSC) ~~vs~~versus green fluorescence (FL1). Heterotrophic bacteria were distinguished from photosynthetic bacteria (*Prochlorococcus* and *Synechococcus*) by their signature in a plot of red fluorescence (FL2) ~~vs~~versus green fluorescence (FL1). Yellow-green latex beads (1 μ m, Polysciences) were used as an internal standard. ~~(Stolle et al., 2009). (Gasol and del Giorgio, 2000).~~ Cell counts were determined with the CellQuest software (Becton Dickinson). For autotrophic pico and nanoplankton <20 μ m, 2 mL samples were fixed with formaldehyde (1 % final concentration) and stored frozen ~~(-80~~(-80 °C) until analysis. Red and orange autofluorescence was used to identify Chl-*a* and phycoerythrin cells. Cell counts were determined with CellQuest software (Becton Dickinson); picoplankton and nanoplankton populations containing Chl-*a* and/or phycoerythrin (i.e., *Synechococcus*) were identified and enumerated. We converted the cell abundance of the different autotrophic ~~plankton~~pico- and nanoplankton populations into biomass assuming 43 fg C cell⁻¹ for *Prochlorococcus*, 120 fg C cell⁻¹ for *Synechococcus*, 500 fg C cell⁻¹ for eukaryotic picoplankton and, 3.100 fg C cell⁻¹ for eukaryotic nanoplankton after Hernández-Hernández et al., ~~(2020).~~ We report the autotrophic ~~plankton~~pico- and nanoplankton biomass as the sum of eukaryotic pico- and nanoplankton and cyanobacteria (*Prochlorococcus* and *Synechococcus*) biomass. The abundance of eukaryotic pico- and nanoplankton and cyanobacteria (*Prochlorococcus* and *Synechococcus*) can be found in the SI (Table S2).

2.3 ~~2.3~~ Microbial activities

~~More information on procedures and calculations of microbial activities are given in the SI. Bacterial biomass production rates (BP) were measured through the incorporation of labeled leucine (³H) (specific activity 100 Ci mmol⁻¹, Biotrend) using the microcentrifuge method (Kirehman et al., 1985; Smith and Azam, 1992). Duplicate samples and one killed control (1.5 mL each) were labeled using ³H-leucine at a final concentration of 20 nmol L⁻¹ and incubated with headspace for 6 h in the dark at 14 °C. Controls were poisoned with trichloroacetic acid. All Samples were measured on board with a liquid scintillation analyzer (Packard Tri-Carb, model 1900 A). ³H-leucine uptake was converted to carbon units applying a conversion factor of 1.55 kg C mol⁻¹ leucine (Simon and Azam, 1989).~~

BP rates at 22 °C were estimated following López-Urrutia and Morán (2007):

$$BP_{22^{\circ}\text{C}} = BP_{14^{\circ}\text{C}} \times 0.996 \text{ (Eq. 1)}$$

Community respiration rates (CR) were estimated from changes of dissolved oxygen in 24–36 hours incubations at 14 °C using optode spot mini sensors (PreSens PST3; Precision Sensing GmbH, Regensburg, Germany). The detection limit (DL) for CR was 0.55 $\mu\text{mol O}_2 \text{ L}^{-1} \text{ d}^{-1}$.

CR at 22 °C was estimated using extrapolation from Regaudie De Gioux and Duarte (2012):

$$CR_{22^{\circ}\text{C}} = CR_{14^{\circ}\text{C}} \times 2.011 - 0.013 \text{ (Eq. 2)}$$

CR_{22°C} was converted into bacterial respiration (BR_{22°C}) after Aranguren-Gassis et al. (2012):

$$BR_{22^{\circ}\text{C}} = 0.30 \times CR_{22^{\circ}\text{C}}^{1.22} - 0.013 \text{ (Eq. 3)}$$

A respiratory quotient of 1 was used to convert oxygen consumption into carbon respiration (del Giorgio and Cole 1998).

We furthermore estimated the bacterial carbon demand (BCD):

$$BCD = BP + BR \text{ (Eq. 4)}$$

and the bacterial growth efficiency (BGE):

$$BGE = \frac{BP}{BCD} \text{ (Eq. 5)}$$

Primary production (PP) was determined from ¹⁴C incorporation according to Steemann Nielsen (1952) and Gargas (1975). Polycarbonate bottles (Nunc EasYFlask, 75 cm²) were filled with 260 mL prefiltered (mesh size of 200 μm) sample and spiked with 50 μL of a $\sim 11 \mu\text{Ci NaH}^{14}\text{CO}_3^-$ solution (Perkin Elmer, Norway). 200 μL were removed immediately after spiking and transferred to a 5 mL scintillation vial for determination of added activity. Then, 50 μL of 2N NaOH and 4 mL scintillation cocktail (Ultima Gold AB) were added. Duplicate samples from the top three depths at selected stations (SI Table S1) were incubated in 12 h light and 12 h dark at 22 °C. Three, which was the average temperature of the upper 100 m depth (22 \pm 3 °C) along the transect. The incubator was set to reproduce three light levels ~~were applied~~: 1200–1400; 350 and 5 μE , with high values representing surface irradiance at the time of sampling. The incubation length was chosen for two reasons. First, we expected low productivity of the open ocean phytoplankton community due to low biomass and low nutrient concentrations at the start of the incubation. Under these conditions, short-term incubations of only a few hours may underestimate PP, because carbon assimilation by algal cells may be too low to

discriminate against ^{14}C adsorption as determined in blank dark incubation (Engel et al., 2013). Moreover, the release of freshly assimilated carbon into the DOM pool has a time scale of several hours because of the equilibration of the tracer and because metabolic processes of organic carbon exudation follow those of carbon fixation inside the cell (Engel et al., 2013). Incubations were stopped by filtration of a 70 mL sub-sample onto 0.4 μm polycarbonate filters (Nuclepore). Particulate primary production (PP_{POC}) was determined from material collected on the filter, while the filtrate was used to determine dissolved primary production (PP_{DOC}). All filters were rinsed with 10 mL sterile filtered ($<0.2 \mu\text{m}$) seawater, and then acidified with 250 μL 2N HCl to remove inorganic carbon (Descy et al., 2002). Filters were transferred into 5 mL scintillation vials, and 4 mL scintillation cocktail (Ultima Gold AB) was added. To determine PP_{POC} and PP_{DOC} , 4 mL of filtrate ~~and incubated sample~~ were transferred to 20 mL scintillation vials, ~~and~~ acidified ~~(with 100 μL 1N HCl), and~~. Scintillation vials were left open in the fume hood for 14 hours to remove inorganic carbon. Then, 100 μL of 2N NaOH and 15 mL scintillation cocktail were added. All samples were counted the following day in a liquid scintillation analyzer (Packard Tri-Carb, model 1900 A).

Primary production (PP) of organic carbon was calculated according to Gargas (1975):

$$\text{PP } (\mu\text{mol C L}^{-1} \text{ d}^{-1}) (\mu\text{mol C L}^{-1} \text{ d}^{-1}) = \frac{a_2 \times \text{DI}^{12}\text{C} \times 1.05 \times k_1 \times k_2}{a_1} \quad (\text{Eq. 61})$$

~~Where~~ where a_1 and a_2 are the activities (DPM) (disintegrations per minute) of the added solution and the sample corrected for dark sample, respectively, and DI^{12}C is the concentration ($\mu\text{mol L}^{-1}$) of dissolved inorganic carbon (DIC) in the sample. ~~Dissolved inorganic carbon~~ DIC concentration was calculated from total alkalinity using ~~the R~~ the R package seacarb (Gattuso et al., 2020). Total alkalinity of the seawater was acquired through the open-cell titration method (Dickson et al., 2007). The value 1.05 is a correction factor for the discrimination between ^{12}C and ^{14}C , as the uptake of the ^{14}C isotope is 5% slower than the uptake of ^{12}C , k_1 is a correction factor for subsampling (bottle volume/filtered volume) and k_2 is the incubation time (d^{-1}). Total primary production (PP_{TOT} ; $\mu\text{mol C L}^{-1} \text{ d}^{-1}$) was derived from the sum of PP_{POC} and PP_{DOC} according to:

$$\text{PP}_{\text{TOT}} = \text{PP}_{\text{POC}} + \text{PP}_{\text{DOC}} \quad (\text{Eq. 72})$$

The percentage of extracellular release (PER; %) was calculated as:

$$PER = \left(\frac{PP_{DOC}}{PP_{TOT}} \right) \times 100 \quad (\text{Eq. 83})$$

Bacterial biomass production rates (BP) were measured through the incorporation of labeled leucine (^3H) (specific activity 100 Ci mmol⁻¹, Biotrend) using the microcentrifuge method (Kirchman et al., 1985; Smith and Azam, 1992). Duplicate samples and one killed control (1.5 mL each) were labeled using ^3H -leucine at a final concentration of 20 nmol L⁻¹. BP was determined down to 800 m depth and, for practical reasons, we chose an incubation temperature of 14 °C as an average over this depth interval. However, in this paper, only data from the top 100 m depth are shown and BP rates were corrected for the difference between incubation and *in situ* temperature (Eq. 4). All samples were incubated for 6 h in the dark with headspace. Controls were poisoned with trichloroacetic acid. All Samples were measured on board with a liquid scintillation analyzer (Packard Tri-Carb, model 1900 A). ^3H -leucine uptake was converted to carbon units by applying a conversion factor of 1.55 kg C mol⁻¹ leucine (Simon and Azam, 1989).

BP rates from incubations at 14 °C were converted to BP rates at 22 °C following the equation from López-Urrutia and Morán (2007):

$$BP_{22^\circ\text{C}} = BP_{14^\circ\text{C}} \times 1.906 \quad (\text{Eq. 4})$$

Community respiration rates (CR) were estimated from quadruplicate incubations by measuring changes of dissolved oxygen over 24-36 hours at the same temperature as used for BP (14 °C) using optode spot mini sensors (PreSens PSt3; Precision Sensing GmbH, Regensburg, Germany). The detection limit (DL) for CR was 0.55 μmol O₂ L⁻¹ d⁻¹.

CR at 22°C was estimated using the extrapolation from Regaudie-De-Gioux and Duarte (2012):

$$CR_{22^\circ\text{C}} = CR_{14^\circ\text{C}} \times 2.011 - 0.013 \quad (\text{Eq. 5})$$

CR_{22°C} was converted into bacterial respiration (BR_{22°C}) after Aranguren-Gassis et al. (2012):

$$BR_{22^\circ\text{C}} = 0.30 \times CR_{22^\circ\text{C}}^{1.22} - 0.013 \quad (\text{Eq. 6})$$

A respiratory quotient of 1 was used to convert oxygen consumption into carbon respiration (del Giorgio and Cole 1998).

We estimated the bacterial carbon demand (BCD) as follows:

$$BCD = BP + BR \quad (\text{Eq. 7})$$

Bacterial growth efficiency (BGE) was calculated from BP and BCD:

$$BGE = \frac{BP}{BCD} \text{ (Eq. 8)}$$

Detailed information on procedures and calculations of microbial activities are provided in the SI.

2.4 Data analysis

Statistical analyses and calculations were conducted using the software R (v4.0.3) in RstudioR studio (v1.1.414; Ihaka and Gentleman 1996). Analysis of variances (ANOVA) and Tukey test, were performed on the different parameters by grouping the station by their position (SI Table ~~4S1~~). Seawater density was calculated using ~~R~~ package oce v1.3.0 (Kelley, 2018) and the mixed layer maximum depth was determined as the depth at which a change from the surface density of 0.125 kg m^{-3} has occurred (Levitus, 1982). ~~Section plots were realized using Ocean Data View (Schlitzer, 2020).~~ Other R packages used in this study include corplot v0.84 (Dray, 2008) and ggplot2 v3.3.3 (Wickham, 2016). Section plots were made using Ocean Data View v5.6.2 (Schlitzer, 2020). Depth integrated values were calculated using the midpoint rule.

3. Results

3.1 Hydrographic conditions

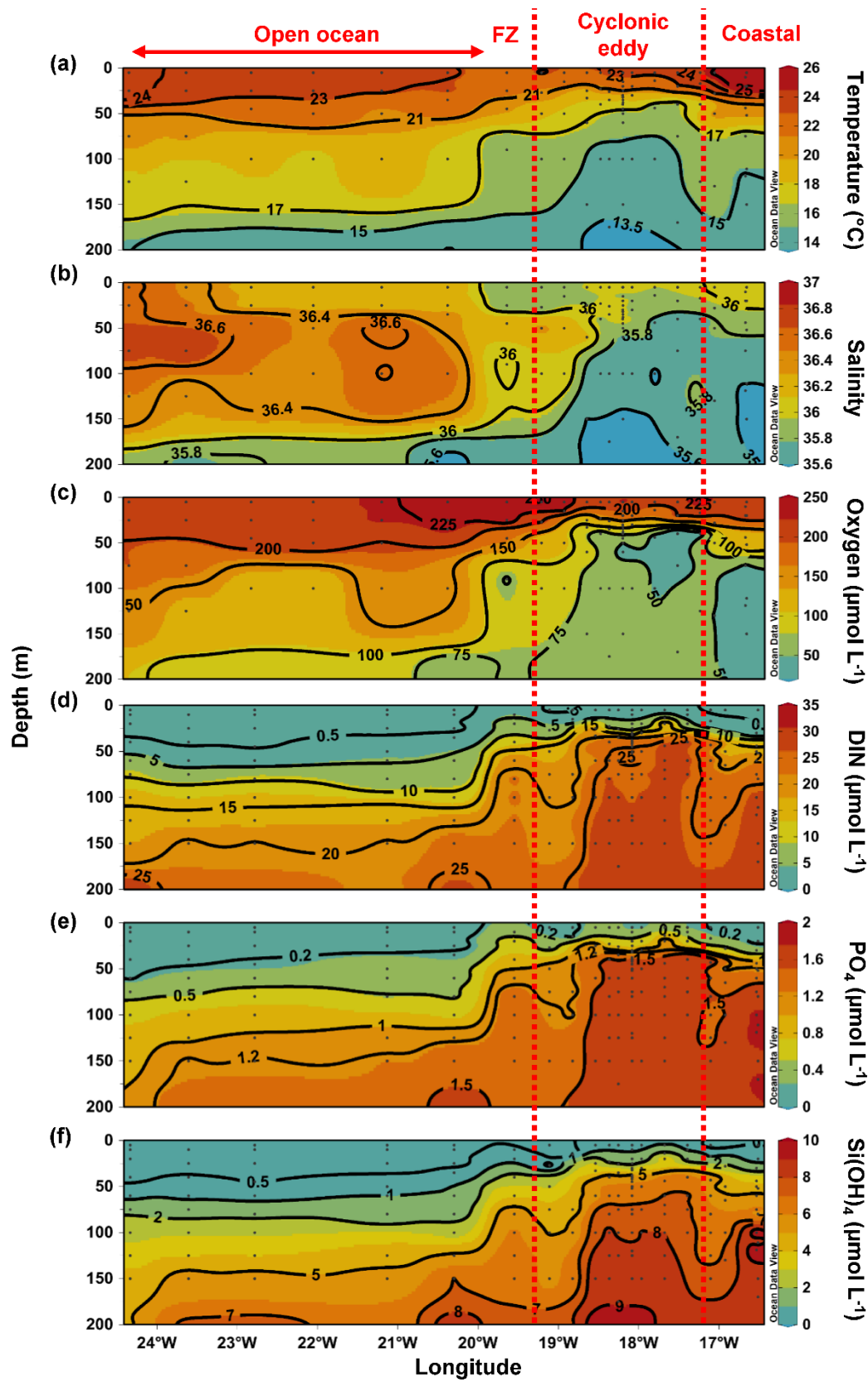
Along the zonal transect, open ocean waters (from 20 to 24.5 °W) had a temperature range of ~~17.0-13.45~~-24.32 °C and a salinity ~~of 36.19~~between 35.55-36.79 in the upper ~~150m~~200 m depth (Fig. ~~2a~~ &and **b**). The average mixed layer depth was $30 \pm 2 \text{ m}$ (Fig. ~~3a~~ SI Table 4S1). Oxygen ~~concentration~~concentrations (Fig. **2c**) decreased with depth while nutrient concentrations increased (Fig. **2d-e**). Nutrients were depleted (<0.5 , <0.2 , and $<0.5 \text{ } \mu\text{mol L}^{-1}$ for DIN, PO_4 , Si(OH)_4 , respectively) in the mixed layer.

At the coastal stations (16.51 to 16.92 °W), the temperature had a range of 14.6-26.1 °C and a salinity ~~of between~~ 35.53- and 36.08 in the upper ~~150~~200 m depth (Fig. ~~2a~~ &and **b**). Here, the mixed layer was significantly shallower than in the open ocean (Tukey, $p < 0.01$), with an average depth of $17 \pm 4 \text{ m}$ (Fig. ~~3a~~ SI Table 4S1). Oxygen was decreasing with depth and a shallow oxygen minimum zone (OMZ; $<50 \text{ } \mu\text{mol kg}^{-1}$) was detected (~~Fig. 2e~~ from between 80 m ~~to and~~ 200 m depth (Fig. 2c)). Nutrients (Fig. **2d-e**) were depleted at the surface (5 m depth), while the deeper coastal waters (~ 80 to 200 m depth) were colder and richer in nutrients than

396 ~~in~~ the open ocean waters, with on average 3.4-fold ~~more nutrients~~ higher nutrient concentrations
397 (DIN, PO₄, Si(OH)₄) when integrated over 100 m depth ~~(data not shown)~~.

398 In the CE ('periphery' and 'core'), waters had a temperature range of 13.52-24.2 °C and a
399 salinity ~~of between~~ 35.48- and 36.36 in the upper ~~150-200~~ m depth (Fig. ~~2a~~ &and ~~b~~). A
400 ~~tightening~~ compression of isopycnals with a strong doming of the isotherms, isohalines, and
401 nutriclines was observed (Fig. ~~2a-b~~, d-f). A shallow OMZ was detected from ~~~30m~~ 30 m to
402 ~100 m depth with the lowest oxygen concentration (<10 µmol kg⁻¹) between 30-40 m ~~depth~~.
403 The mixed layer was significantly shallower (Tukey, $p < 0.05$) ~~at in~~ the CE periphery than in ~~the~~
404 ~~open ocean~~ all other stations, with an average of 15 ± 6 m depth ~~(Fig. 3a)~~. However, the CE
405 core was not significantly different ~~(21 ± 3 from the open ocean (20 ± 2 m; Tukey, $p > 0.05$).~~
406 ~~Nutrients (Fig. 2d-f)~~ At the surface (5 m depth), nutrients were depleted (<0.5, <0.2 and <0.5
407 µmol L⁻¹ for DIN, PO₄, Si(OH)₄, respectively) ~~at the surface (~5 m)~~ only in the ~~Easternmost~~
408 eastern (17.11 °W, 18 °N) and ~~Western~~ western (18.83-19.11 °W, 18.58 °N) part of the CE
409 periphery (Fig. 2d-f). In the core, nutrient concentrations were also lowest in the surface water,
410 but richer in nutrients than in the ambient waters.

411 The Frontal Zone station E3 (19.55 °W) was distinct from the adjacent stations with respect to
412 surface temperature (1 °C colder, Fig 2a). A doming of the nutriclines was observed (Fig. 2d-f)
413 and nutrient concentrations integrated over 100 m depth at St. E3 were ~3 fold higher than
414 ~~Open at the open~~ ocean ~~St.~~ S4 (20.3 °W) and ~1.2 fold higher than at the CE periphery St. EDZ-
415 1 (19.11 °W).



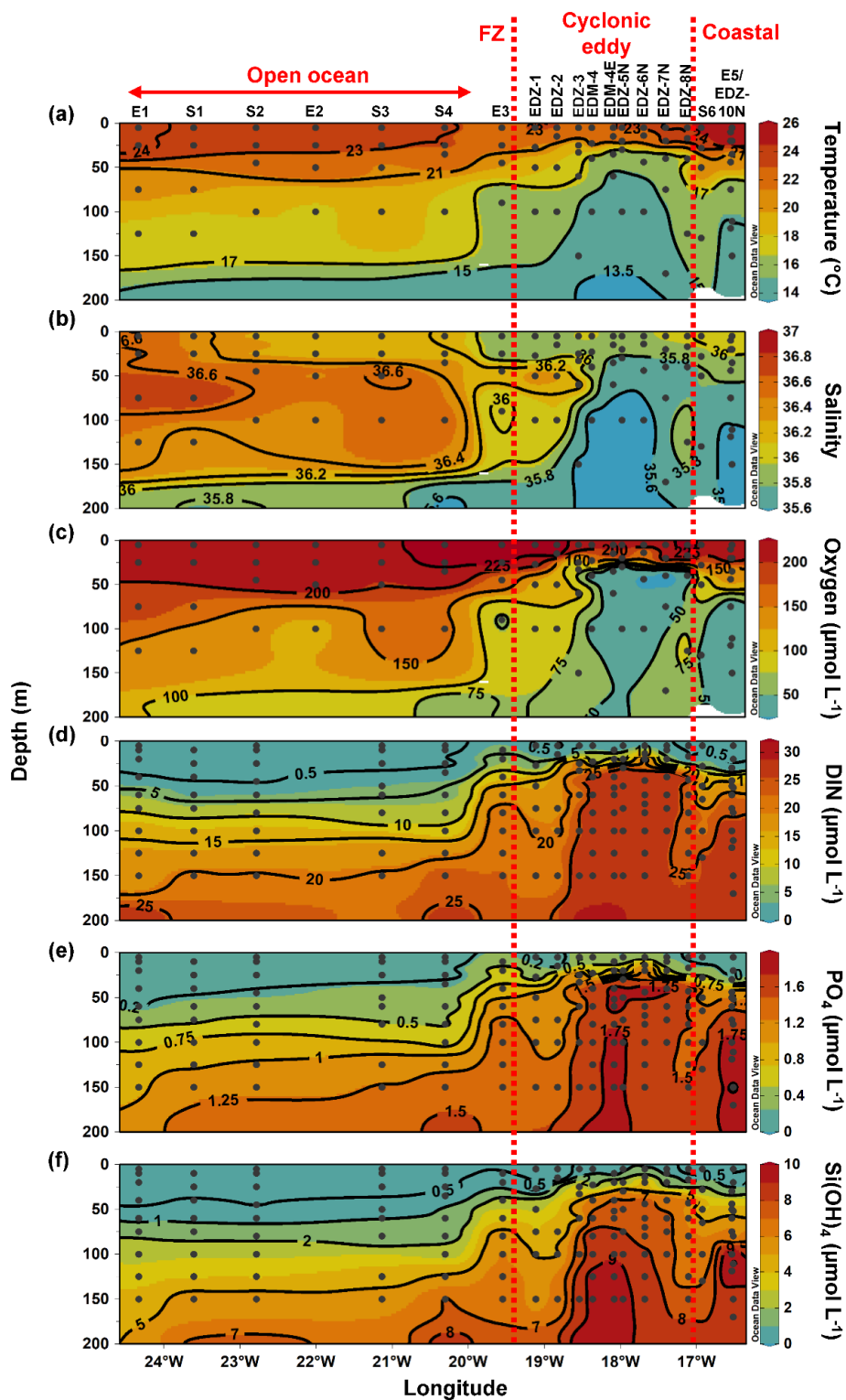


Figure 2: Epipelagic distribution (0-200m) of Temperature (a), Salinity (b), Oxygen (c), Total inorganic nitrogen (DIN) (d), phosphate (PO_4) (e), and silicate (Si(OH)_4) (f). Red dashed lines show the western and eastern boundary of the cyclonic eddy periphery and, respectively. FZ refers to Frontal Zone.

3.2 Chlorophyll-*a* and primary production

In order to compare stations along the zonal transect and within the eddy, data were integrated over the water column (0-100 m depth). Along the zonal transect, depth-integrated Chl-*a* concentration ranged between 11.7 and 58.7 mg m⁻² and decreased from the coastal to the open ocean stations (Table 1; SI-Fig. S43b). Depth-distribution (Fig. 3a) presented showed a Chl-*a* maximum in the open ocean around ~75 m from 23.61 to 24.33 °W and around ~50 m from 22.78 to 20.3 °W, up to 0.7068 µg L⁻¹ (Fig. 4a). At the coastal stations, the Chl-*a* maximum was found between 30-40 m depth with values up to 0.96 µg L⁻¹. Integrated biomass of autotrophic plankton pico-and nanoplankton (Table 1) ranged between 1.6 and 7.8 and between 3.6 and 6.1 g C m⁻² in the open ocean and at the coastal stations, respectively. In the open ocean waters, the depth distribution of autotrophic plankton pico-and nanoplankton biomass (Fig. 3b) presented showed a gradient of distribution from west to east with a concentration maximum around at ~75 m from 23.61 to 24.33 °W, around a concentrations maximum at ~50 m from 22 to 22.78 °W, and a concentrations maximum between 5-25 m from 21.13 to 20.3 °W, with values. Concentrations reached up to 166 µg C L⁻¹. In At the coastal stations, the maximum autotrophic plankton pico-and nanoplankton biomass maximum was found between 30-40 m depth with values up to 117 µg C L⁻¹. Both Chl-*a* concentration and autotrophic plankton pico-and nanoplankton biomass did not vary significantly between the open ocean and the coastal stations (Tukey, $p > 0.05$). Integrated total and dissolved primary production (PP_{TOT}; PP_{DOC}; Table 1) remained fairly constant with ranges of 101-137 and 42.8-78 mmol C m⁻² d⁻¹, respectively, from at the coastal to and the open ocean stations, except for. An exception was the station furthest offshore (24.33 °W), where rates decreased sharply to 25.8 mmol C m⁻² d⁻¹ for PP_{TOT} and to 12.3 mmol C m⁻² d⁻¹ for PP_{DOC}. The integrated percentage of extracellular release (PER; Table 1) in both regions ranged between 42.3- and 67.5%. Both PP_{TOT} and PP_{DOC} and PER did not vary significantly between the open ocean and the coastal stations (Tukey, $p > 0.05$). PP_{TOT} was decreasing and PP_{DOC} decreased with depth except for station E2 (Fig. 3e) 4c, while PER was increasing increased (Fig. 3d). In general, PP_{TOT} and PP_{DOC} were positively correlated to the Chl-*a* concentration ($R^2 = 0.48$ and 0.42 respectively; $p < 0.001$; Fig. 6e & d) 4d).

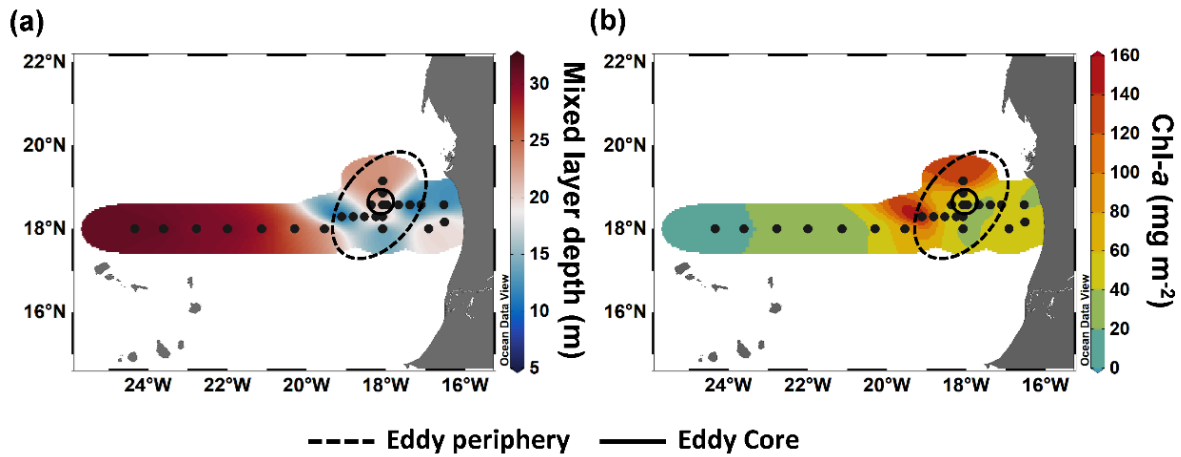


Figure 3: Spatial distribution of maximum mixed layer depth (a) and integrated chlorophyll *a* (Chl-*a*) over 100 m depth (b) during M156.

In the CE (core and periphery) and at the Frontal Zone, integrated Chl-*a* concentration ranged from 17.2 to 225 mg m⁻² (Table 1). The Chl-*a* distribution (SI Fig. S43a) showed a clear spatial separation with the highest values (98.7-225 mg m⁻²) in the western (18.83-19.11 °W, 18.29 °N) and northern (148 mg m⁻²; 18.08 °W, 19.15 °N) parts of the CE and lowest values (26.8-37.5 mg m⁻²) in the southern and eastern in the Southern (18.08 °W, 18 °N) and Eastern part (17.39-17.68 °W, 18.58 °N) part. Depth distribution of Chl-*a* concentration also differed across the eddy, with values >0.5 µg L⁻¹ reaching down to 45 m depth at the Frontal Zone and the western part of the CE (19.11-19.55 °W) and down to 30 m depth in the eastern sidepart of the CE (Fig. 4a). Highest concentrations were detected in the western part of the eddy with 8.7 µg L⁻¹ (17.4 °W) at station EDZ-1 at 27 m. Within the upper 30 m, Chl-*a* concentration within the CE was significantly higher than at the open ocean and the coastal stations (ANOVA, $p < 0.05$). Integrated autotrophic plankton pico- and nanoplankton biomass ranged between 0.3 and 4.7 g C m⁻² in the CE (Table 1). Depth distribution of autotrophic plankton pico- and nanoplankton biomass (Fig. 3b4b) showed low biomass in the upper 40 m (<25 µg C L⁻¹) from 18.83 to 19.11 °W. In contrast, higher biomass (>25 µg C L⁻¹) occurred in the more eastern stations of the CE (17.11 to 18.54 °W) and westwards from the Frontal Zone (19.55 °W). In the eddy, autotrophic plankton pico- and nanoplankton biomass reached higher concentrations mostly mainly within the upper 40 m, with values up to 191 µg C L⁻¹. It should be noted that autotrophic biomass refers only to pico- and nanophytoplankton and not to larger cells such as typical for diatoms or dinoflagellates. Depth-integrated PP_{TOT} and PP_{DOC} rates were significantly higher in the CE and at the Frontal Zone than at the open ocean and the coastal stations (Tukey, $p < 0.05$) with values ranging from 245 to 687 mmol C m⁻² d⁻¹ and from 95.9 to 238 mmol C m⁻² d⁻¹, respectively (Table 1). PP_{TOT} rates (Fig. 2e4c; Table 2) were fairly constant

across the CE's surface (5 m depth), ranging between 11.7 to 2 and 13.37 $\mu\text{mol C L}^{-1} \text{ d}^{-1}$, but varied strongly between 15-40 m depth with values from (0.2 to 14.5 $\mu\text{mol C L}^{-1} \text{ d}^{-1}$). The highest PP_{TOT} rates were found in the Frontal Zone with up to 25.0 $\mu\text{mol C L}^{-1} \text{ d}^{-1}$ at the surface. The range of PP_{DOC} rates (Table 2; Fig. 4d) was larger in the CE (0.2-4.9 $\mu\text{mol C L}^{-1} \text{ d}^{-1}$) and the Frontal Zone (0.7-7.8 $\mu\text{mol C L}^{-1} \text{ d}^{-1}$) than in the open ocean and at the coastal stations. Integrated PER had a range of 29.4-43.340.8 % (Table 1). Compared to open ocean and coastal stations, a slightly lower PER was observed within the upper 40 m (Fig. 2d4e) for the CE and Frontal Zone compared to open ocean and coastal stations.

Table 1: Chlorophyll a (Chl a) and abundance, biomass and activity of phyto and bacterial plankton, integrated over the upper 100m depth. '-' indicate that the parameter was not measured. PP_{DOC} and PP_{TOT} rates in St EDM-4E were measured on the 22/07/2019 from 5, 33 and 50m depth and CR and BR rates were measured in St. E5 on the 29/07/2019 from 5, 35 and 50m depth.

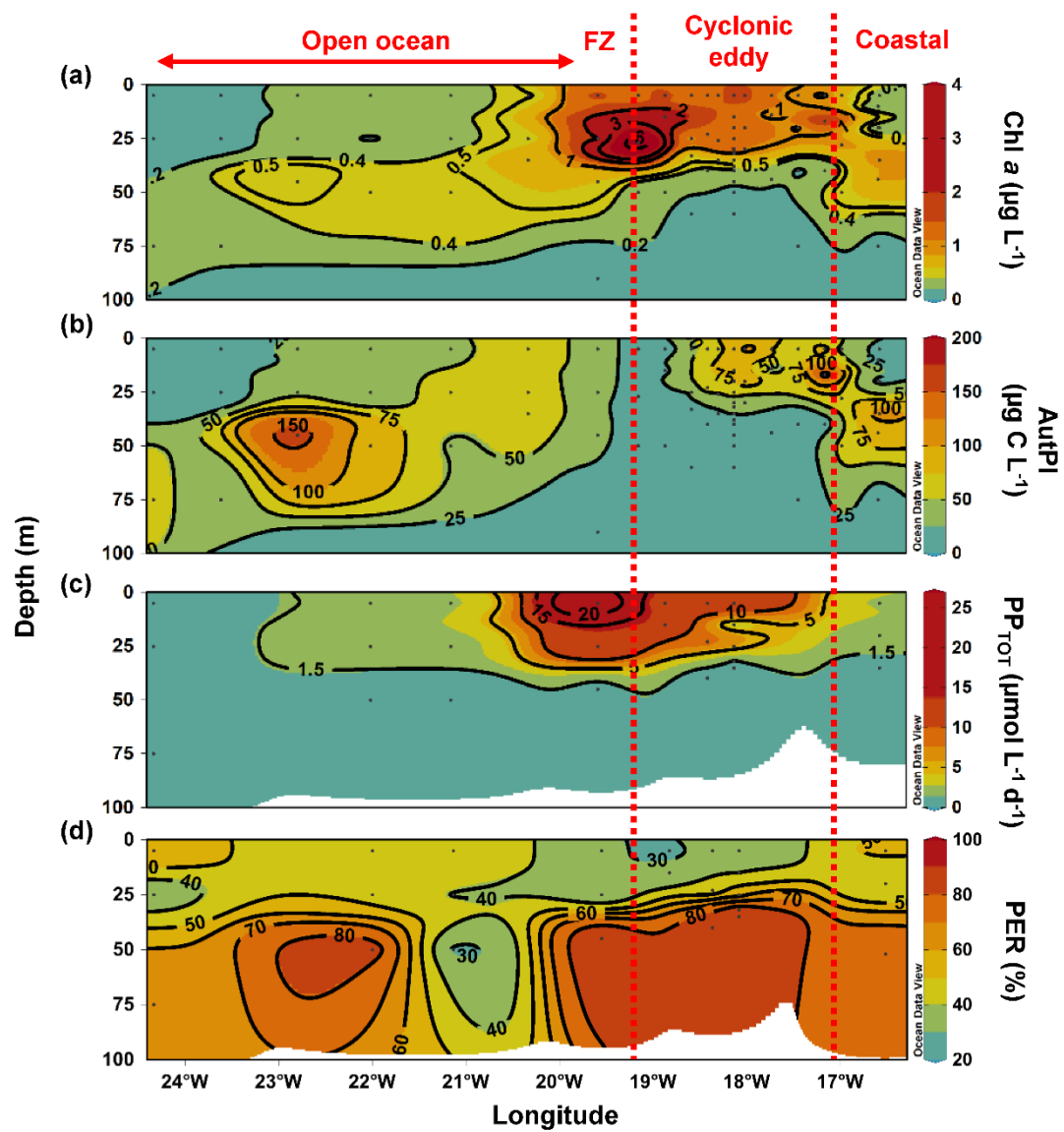
Location	Station	Chl a (mg m^{-2})	AutPI (g C m^{-2})	PP_{DOC} ($\text{mmol C m}^{-2} \text{ d}^{-1}$)	PP_{TOT} ($\text{mmol C m}^{-2} \text{ d}^{-1}$)	PER (%)	HB (10^{15} cell m^{-2})	CR ($\text{mmol C m}^{-2} \text{ d}^{-1}$)	BR ($\text{mmol C m}^{-2} \text{ d}^{-1}$)	BP ($\text{mmol C m}^{-2} \text{ d}^{-1}$)
Coastal	E5	54.5	6.1	75.2	137	54.9	14.7	99.6	32	2.9
	EDZ-10N	36.8	3.6	-	-	-	13.8	-	-	4.1
	AZM-3	58.7	5.3	-	-	-	12.9	-	-	5.7
Eddy Periphery	EDZ-8N	61.5	4.7	-	-	-	10.7	-	-	8.2
	EDZ-7N	26.8	1.6	-	-	-	9.4	-	-	5.7
	EDZ-6N	27.9	1.2	-	-	-	9.1	-	-	4.0
Eddy Core	EDZ-5N	39.2	4.1	-	-	-	14.5	154	59.1	4.7

Table 1 cont.: Chlorophyll a (Chl

Location	Station	Chl <i>a</i> (mg m ⁻²)	AutPI (g C m ⁻²)	PP _{DOC} (mmol C m ⁻² d ⁻¹)	PP _{TOT} (mmol C m ⁻² d ⁻¹)	PE R (%)	HB (10 ¹⁵ cell m ⁻²)	CR (mmol C m ⁻² d ⁻¹)	BR (mmol C m ⁻² d ⁻¹)	BP (mmol C m ⁻² d ⁻¹)
Eddy Core	EDM-4E	46.0	3.3	95.9	245	39.2	15.2	135	60.8	4.5
	EDM-3E	77.5	3.2	-	-	-	15.3	-	-	8.6
	EDM-4	63.8	3.3	141	380	37.2	19.4	275	127	6.4
Eddy Peripher y	S5	35.7	3.6	117	288	40.8	23.7	-	-	6.8
	EDM-5E	35.2	1.6	-	-	-	11.8	-	-	4.7
	EDM-2E	148	1.7	-	-	-	20.8	-	-	11.4
	EDZ-4	47.8	1.0	-	-	-	14.4	-	-	6.3
	EDZ-3	17.2	0.3	-	-	-	9.6	-	-	2.9
	EDZ-2	98.7	0.7	131	445	29.4	8.2	592	320	8.1
	EDZ-1	225	0.6	-	-	-	13.7	-	-	19.3
Frontal Zone	E3	72.1	2.4	238	687	34.6	12.9	529	257	7.7
Open ocean	S4	40.2	4.5	-	-	-	16.9	-	-	4.3
	S3	30.7	4.0	42.8	101	42.3	14.5	346	148	2.6
	E2	22.3	4.4	78.0	116	67.5	12.2	387	168	2.3
	S2	34.1	7.8	-	-	-	13.9	-	-	2.1
	S1	12.2	1.6	-	-	-	5.4	-	-	0.7
	E1	11.7	2.3	12.3	25.8	47.6	6.7	19.7	6.3	0.8

Table 1: Chlorophyll *a* (Chl-*a*) and abundance, biomass and activity of phyto- and bacterial plankton, integrated over the upper 100m depth. ‘-’ indicate that the parameter/variable was not measured. PP_{DOC} and PP_{TOT} rates in St EDM-4E were measured on the 22/07/2019 from 5, 33 and 50m depth and CR and BR rates were measured in St. E5 on the 29/07/2019 from 5, 35 and 50m depth. can be found in SI Table S1.

Location	Station	Chl- <i>a</i> (mg m ⁻²)	Autpico- nanoPI (g C m ⁻²)	PP _{DOC} (mmol C m ⁻² d ⁻¹)	PP _{TOT} (mmol C m ⁻² d ⁻¹)	PE R (%)	HB (10 ¹⁵ cell m ⁻²)	CR (mmol C m ⁻² d ⁻¹)	BR (mmol C m ⁻² d ⁻¹)	BP (mmol C m ⁻² d ⁻¹)
Coastal	E5	54.5	6.1	75.2	137	54.9	14.7	99.6	32	5.6
	EDZ-10N	36.8	3.6	-	-	-	13.8	-	-	7.9
	AZM-3	58.7	5.3	-	-	-	12.9	-	-	10.8
Eddy Periphery	EDZ-8N	61.5	4.7	-	-	-	10.7	-	-	15.6
	EDZ-7N	26.8	1.6	-	-	-	9.4	-	-	10.8
	EDZ-6N	27.9	1.2	-	-	-	9.1	-	-	7.5
Eddy Core	EDZ-5N	39.2	4.1	-	-	-	14.5	154	59.1	9.0
	EDM-4E	46.0	3.3	95.9	245	39.2	15.2	135	60.8	8.6
	EDM-3E	77.5	3.2	-	-	-	15.3	-	-	16.4
Eddy Periphery	EDM-4	63.8	3.3	141	380	37.2	19.4	275	127	12.2
	EDM-6E	35.7	3.6	117	288	40.8	23.7	-	-	13.0
	EDM-5E	35.2	1.6	-	-	-	11.8	-	-	9.0
	EDM-2E	148	1.7	-	-	-	20.8	-	-	21.8
	EDZ-4	47.8	1.0	-	-	-	14.4	-	-	12.0
	EDZ-3	17.2	0.3	-	-	-	9.6	-	-	5.6
	EDZ-2	98.7	0.7	131	445	29.4	8.2	592	320	15.5
	EDZ-1	225	0.6	-	-	-	13.7	-	-	36.7
Frontal Zone	E3	72.1	2.4	238	687	34.6	12.9	529	257	14.7
Open ocean	S4	40.2	4.5	-	-	-	16.9	-	-	8.2
	S3	30.7	4.0	42.8	101	42.3	14.5	346	148	5.0
	E2	22.3	4.4	78.0	116	67.5	12.2	387	168	3.9
	S2	34.1	7.8	-	-	-	13.9	-	-	4.4
	S1	12.2	1.6	-	-	-	5.4	-	-	1.4
	E1	11.7	2.3	12.3	25.8	47.6	6.7	19.7	6.3	1.6



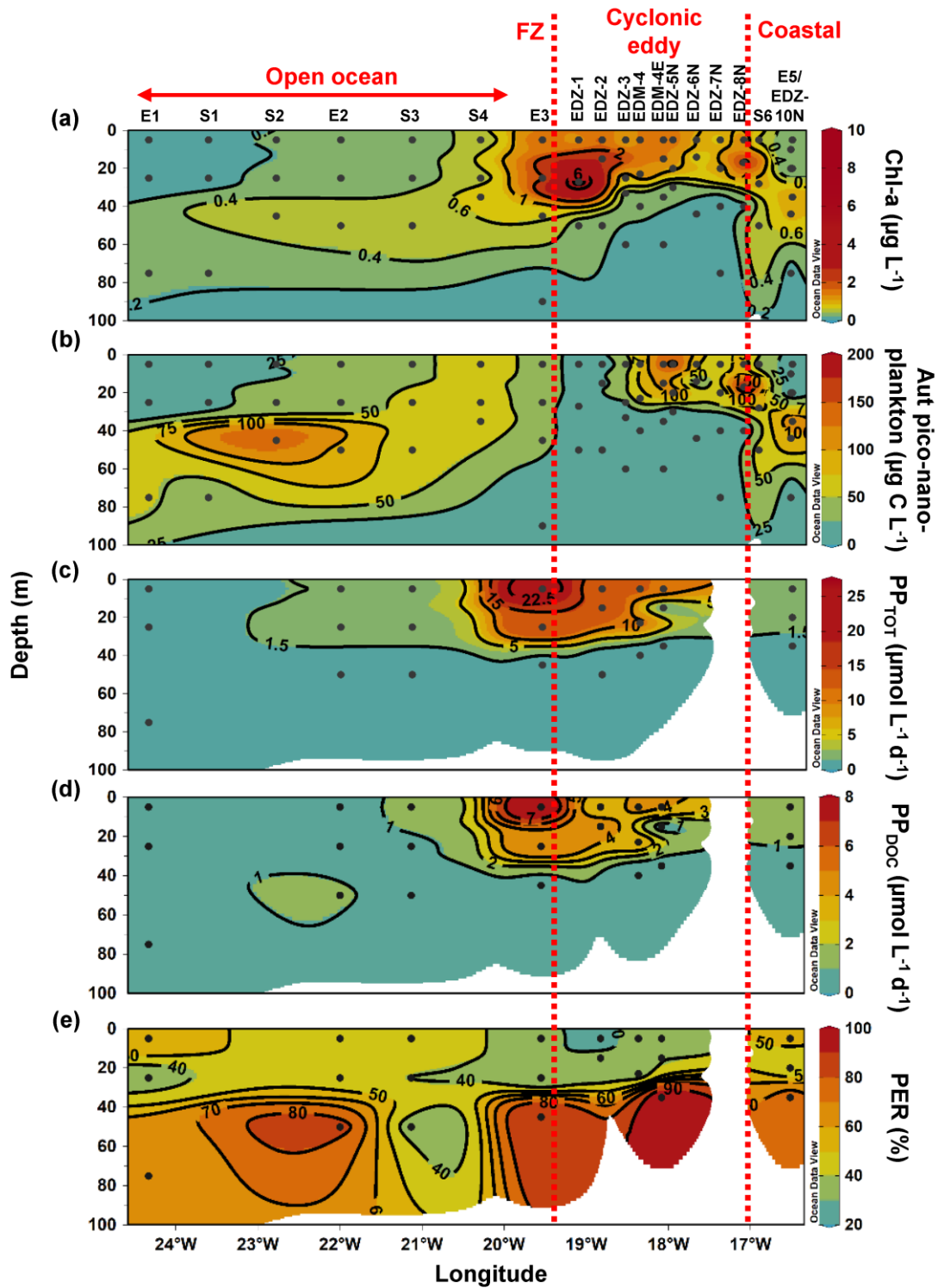


Figure 34: Depth distribution of phytoplankton biomass and activity over 100 m depth, from the surface to 100 m. Chlorophyll *a* (Chl-*a*; a), Autotrophic plankton biomass (Autotrophic plankton; b), total primary production (PP_{TOT} ; c), dissolved primary production (PP_{DOC} ; d) and percentage of extracellular release (PER; e). Red dashed lines show the western and eastern

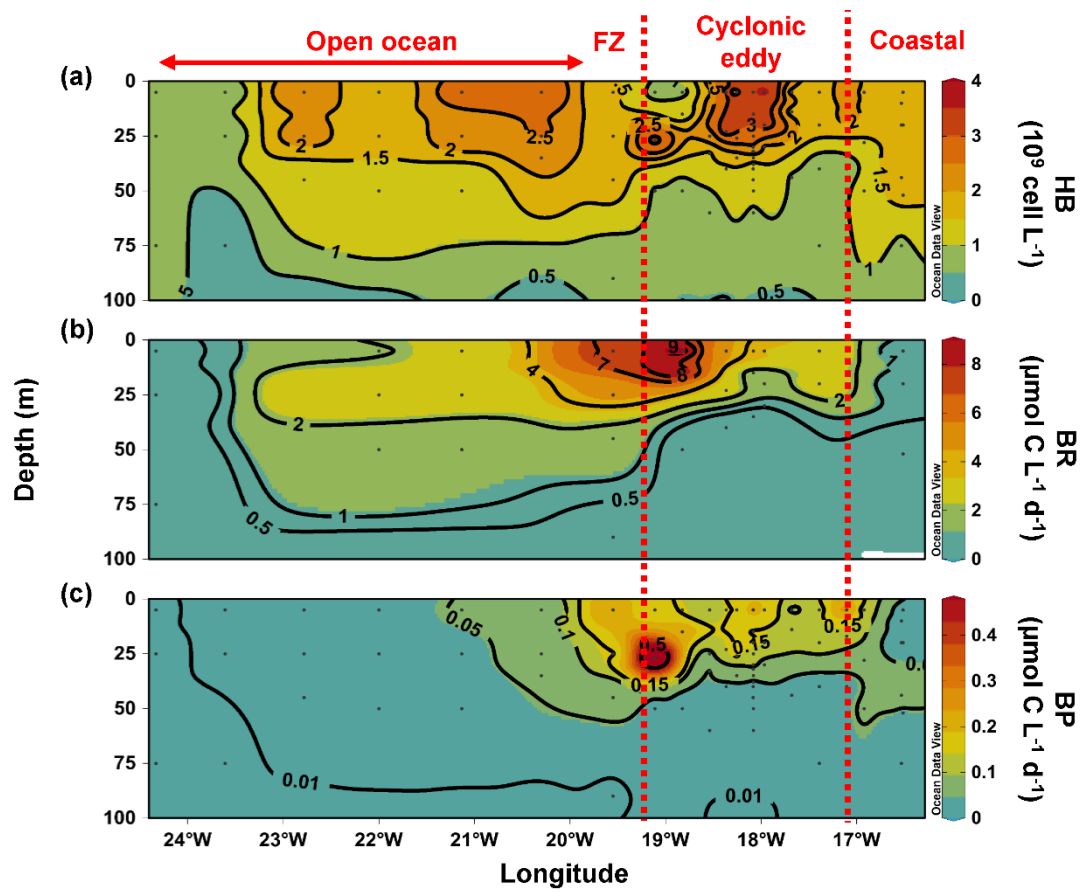
~~boundary of the cyclonic eddy-influenced area and periphery, respectively.~~ FZ ~~refer as~~ refers to Frontal Zone.

3.3 Bacterial abundance and activities

Heterotrophic bacterial abundance decreased with depth and was highest in the upper 50 m ~~of~~ at all stations (Fig. ~~4a~~5a). At the coastal and open ocean stations, integrated (0-100 m ~~depth~~) heterotrophic bacteria abundance ranged between 12.9-14.7 and 5.4-16.9x10¹⁵ cells m⁻², respectively (Table 1). No significant differences in heterotrophic bacterial abundance were observed between the open ocean and coastal stations (Tukey, $p > 0.05$). In the open ocean waters, the lowest integrated BR and CR rates (~~Table 1~~) were ~~reported~~observed at the station furthest offshore (~~24.33 °WE~~1), with 6.3 and 19.7 mmol C m⁻² d⁻¹, respectively. ~~Yet in (Table 1).~~ At the other open ocean stations (~~21.13 to 22 °W~~), integrated BR and CR rates ~~were higher (ranged between 148-168 mmol C m⁻² d⁻¹ and 346-348 mmol C m⁻² d⁻¹, respectively), which was higher than in~~ at the coastal station (~~with BR rates of 32 and mmol C m⁻² d⁻¹ and CR rates of 98 mmol C m⁻² d⁻¹ respectively).~~ Overall, BR and CR rates were higher in the open ocean stations than ~~at in~~ the coastal ~~stations~~ones with ~~high~~highest rates (> 1 and > 2.5 μmol C L⁻¹ d⁻¹, respectively) ~~down to in the top 60 m depth~~ (Fig. ~~4b~~5b; SI Fig. ~~S5a~~S4a). Integrated BP, in contrast, was generally higher at the coastal stations with ~~2.9-5.76-10.8~~ mmol C m⁻² d⁻¹ compared to the open ocean ~~ones~~ with ~~0.7-1.4-3-8.2~~ mmol C m⁻² d⁻¹ (Table 1). However, ~~volumetric~~ BP rates were not significantly different from the open ocean (Tukey $p > 0.05$), where BP rates were more variable. At the coastal stations, the highest BP (~~Fig. 4b~~) rates were observed ~~either~~ at the surface (5 m) ~~and/or at~~ around ~40 m depth, while in the open ocean, the highest rates were ~~constantly~~ found ~~at in~~ the surface (~~5 m samples (Fig. 5c)~~). BGE was determined for the upper 50 m (~~Table 2~~) and showed ~~only~~ little variability ~~over with~~ depth. (~~Table 2; Fig. 5d~~). However, BGE was significantly higher (Tukey, $p < 0.05$) at the coastal ~~than at the open ocean~~ stations ~~with ranges of 5.-(9.6 ± 3 ± 2.2.7% to 8.0 ± 14.1.0% ± 1.7%)~~ compared to ~~0.9 the open ocean ones (1.7 ± 0.1 to 4.2 ± 0.04 to 2.3 ± 0.02%, respectively.%).~~ We estimated the predominance of autotrophy/heterotrophy in the system, by dividing the PP_{TOT} rates by ~~the BCD-CR (Mouriño-Carballido and McGillicuddy 2006).~~ Heterotrophic conditions ($\frac{PP_{TOT}}{BCD} \frac{PP_{TOT}}{CR} < 1$) occurred at the open ocean stations throughout the water column, while autotrophic conditions ($\frac{PP_{TOT}}{BCD} \frac{PP_{TOT}}{CR} > 1$) prevailed at the coastal St. E5 ($\frac{PP_{TOT}}{CR}$ ~~ratio ranging from 0.7 to 1.9;~~ Table 2). This pattern was preserved when data were integrated over the mixed layer (Fig. ~~5~~)

apart for the furthest station offshore (24.33 °W) where autotrophy occurred, yet lower than at the coastal station St.E5 ($\frac{PP_{TOT}}{BCD} = 2$ and 5.5 respectively). PP_{DOC} rates were sufficient to satisfy the BCD at the coastal St. E5, but not in the open ocean stations (Table 2).

In the CE and at the Frontal Zone, integrated heterotrophic bacterial abundance ranged from $8.2\text{--}23.7 \times 10^{15}$ cells m^{-2} (Table 1). In the CE, substantial variation of bacterial abundance occurred within the upper 20 m (Fig. 4a, 5a), with an abundance of $<1 \times 10^9$ cells L^{-1} in the western CE periphery (18.83 to 19.11 °W) of the CE and $> 3 \times 10^9$ cells L^{-1} in the CE core stations (~18 °W). Depth-integrated BR and CR (Table 1) ranged between 59.1 and 320 and between 135 and 592 $mmol\ C\ m^{-2}\ d^{-1}$, respectively (Table 1). Elevated BR and CR rates (> 1 and $2.5\ \mu mol\ C\ L^{-1}\ d^{-1}$, respectively) were only present in the upper ~30-40 m of the CE (Fig. 4b5b; SI Fig. S5aS4a). Integrated BP rates ranged from 2.95.6 to 49.336.7 $mmol\ C\ m^{-2}\ d^{-1}$ in the CE and at the Frontal Zone stations (Table 1). BP rates were elevated in the upper 40 m of the CE and at the Frontal Zone were elevated but were, and significantly higher than in the majority of the coastal and open ocean stations only in the stations within the CE periphery (Tukey $p < 0.05$). Stations in the core of the CE had BGEs (Table 2; Fig. 5d) significantly higher than at the stations located in the open ocean (Tukey, $p < 0.05$). BGE had a range of $1.42.7 \pm 2.29$ to $10.5 \pm 18.3 \pm 1.0$, % and 5% and $2.8.1 \pm 0.12$ to $3.0 \pm 1.75.5 \pm 2.4$ % in the CE and the Frontal Zone stations, respectively. Highest BGE was observed below 20 at 15 m depth in the CE core (up to 10.4818.3%, St. EDM-4E). With ratios ranging from 1.13 to 3.5, the upper 40 m of the CE and the CE and Frontal Zone stations were rather autotrophieshowed net hetero- as well as net autotrophy (Table 2), with a $\frac{PP_{TOT}}{CR}$ ratio ranging from 0.2 to 1.9. When integrated over the mixed layer (Fig. 56), stations within the core of the CE and at the Frontal Zone were net autotrophic, with a $\frac{PP_{TOT}}{BCD} \frac{PP_{TOT}}{CR}$ ratio ranging from 1.17 to 3.8.42 to 1.85, while net heterotrophy occurred at the eddy periphery. PP_{DOC} was on average 70equivalent to 71% of the BCD within the CE and at the Frontal Zone, yet ranging from 28.327.9 to 114.5%.110% (Table 2).



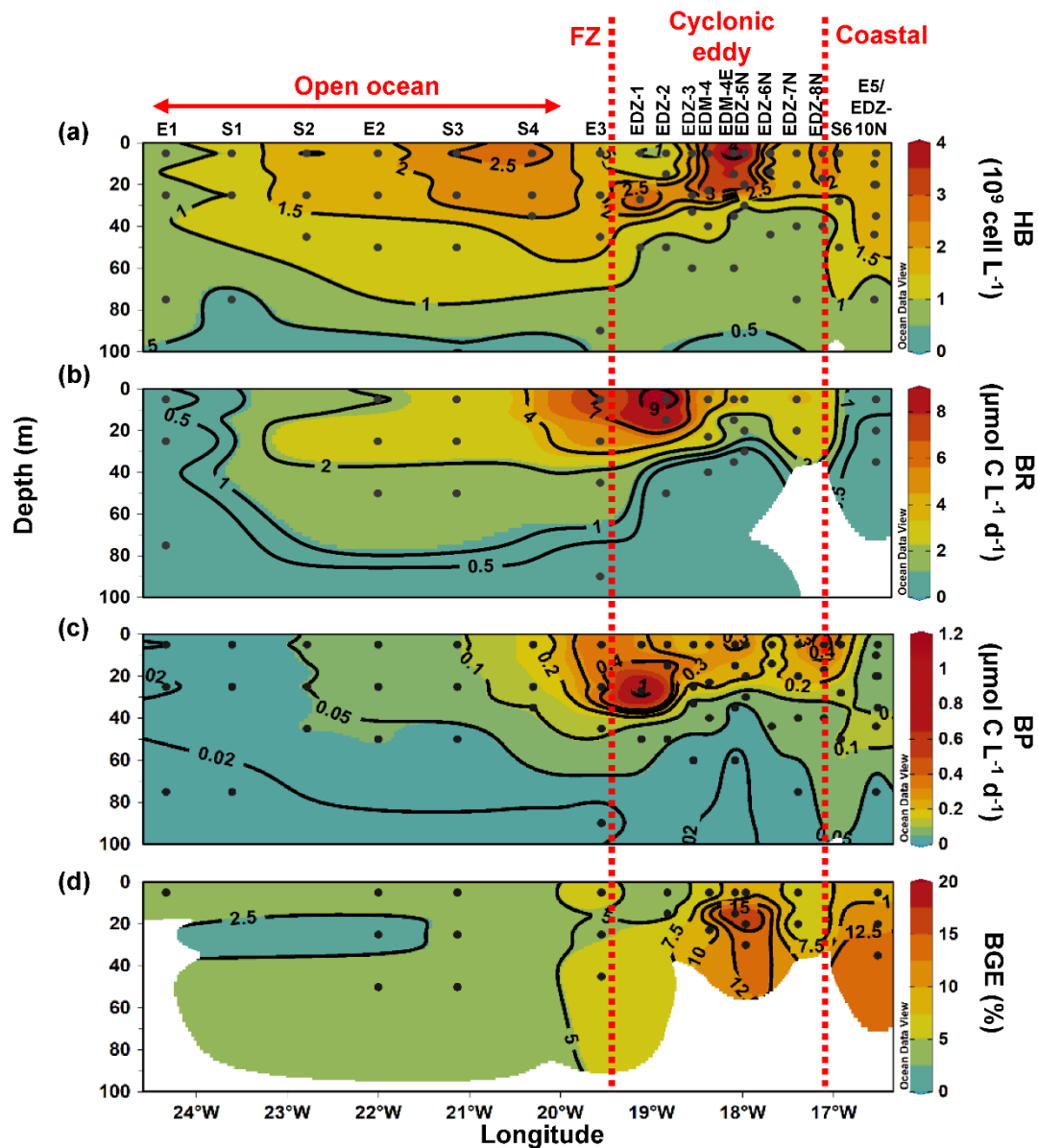


Figure 45: Depth distribution of heterotrophic bacterial abundance and microbial activities over 100m depth from the surface to 100 m. Heterotrophic bacterial abundance (HB; **a**), bacterial respiration (BR; **b**), bacterial production (BP; **c**). Red dashed line show the eddy-influenced area and FZ refers to Frontal Zone), bacterial growth efficiency (BGE; **d**). Red dashed lines show the western and eastern boundary of the cyclonic eddy periphery, respectively. FZ refers to Frontal Zone. BP and CR rates at *in-situ* temperature were estimated based on López-Urrutia and Morán (2007) and on Regaudie-de-Gioux and Duarte (2012). BR rates were estimated from measured and temperature-corrected CR rates based on Aranguren-Gassis et al, (2012). Details are provided in the methods section and the SI.

Table 2: Average (mean) \pm standard deviation of microbial metabolic activities during M156: bacterial carbon demand (BCD); bacterial growth efficiency (BGE); dissolved primary production (PP_{DOC}); Percentage of extracellular release (PER); total primary production (PP_{TOT}) and, the ratio between PP_{DOC} and BCD ($\frac{PP_{DOC}}{BCD}$) and the ratio between PP_{TOT} ($\frac{BCD}{PP_{TOT}}$) and CR ($\frac{PP_{TOT}}{CR}$). BCD and BGE were obtained from temperature-corrected BP and BR rates at 22°C (see text). ‘-’ indicate that the parameter was not measured and ‘B.D.’ below detection (see text). PP_{DOC} and PP_{TOT} rates in St. EDM-4E were measured on the 22/07/2019 from 5, 33 Sampling date, time and 50m depth and CR and BR rates were measured in St. E5 on the 29/07/2019 from 5, 35 and 50m depth are given in SI Table S1.

Location	Station	Depth (m)	BCD ($\mu\text{mol C L}^{-1} \text{d}^{-1}$)	BGE (%)	PP _{DOC} ($\mu\text{mol C L}^{-1} \text{d}^{-1}$)	PER (%)	PP _{TOT} ($\mu\text{mol C L}^{-1} \text{d}^{-1}$)	$\frac{BCD}{PP_{TOT}}$
Coastal	E5	5	0.6 ± 0.1	5.3 ± 2.2	1.5 ± 0.2	34.9 ± 1.1	2.7 ± 0.2	4.5 ± 1.5
		20	0.5 ± 0.1	6.9 ± 1.6	1.2 ± 0.1	52.6 ± 2.7	2.5 ± 0.1	5.5 ± 1.4
		35	0.5 ± 0.3	8.0 ± 1.0	0.7 ± 0.1	89.8 ± 3.9	1.0 ± 0.1	2.1 ± 0.2
Eddy Periphery	EDZ-10N S6	All	-	-	-	-	-	-
		All	-	-	-	-	-	-
	EDZ-8N	All	-	-	-	-	-	-
	EDZ-7N	5	3.5 ± 0.7	3.6 ± 0.3	-	-	-	-
		20	3.5 ± 0.3	3.3 ± 1.7	-	-	-	-
	EDZ-6N	All	-	-	-	-	-	-
Eddy Core	EDZ-5N	5	2.6 ± 0.4	6.02 ± 1.5	-	-	-	-
		20	1.15 ± 0.3	9.51 ± 2.1	-	-	-	-
		30	0.41 ± 0.6	7.11 ± 0.2	-	-	-	-
		100	B.D.	B.D.	-	-	-	-
	EDM-4E	5	4.5 ± 0.4	4.1 ± 1.1	4.3 ± 0.1	36.7 ± 0.2	11.2 ± 0.1	2.5 ± 0.2
		15	1.3 ± 0.4	10.5 ± 0.6	0.4 ± 0.1	39.3 ± 6.8	1.1 ± 0.1	2.1 ± 0.4
		35	B.D.	B.D.	0.6 ± 0.3	94.4 ± 0.9	0.6 ± 0.3	-
		60	B.D.	B.D.	-	-	-	-
	EDM-3E	All	-	-	-	-	-	-
	EDM-4	5	4.7 ± 1.1	3.2 ± 1.4	4.3 ± 1.0	35.1 ± 5.7	12.6 ± 1.2	2.7 ± 1.1
23		3.4 ± 0.2	4.4 ± 2.1	3.9 ± 0.2	35.7 ± 1.4	11.0 ± 0.3	3.2 ± 1.4	
40		B.D.	B.D.	0.3 ± 0.1	85.3 ± 7.1	0.3 ± 0.1	-	
100		B.D.	B.D.	-	-	-	-	
Eddy Periphery	S5	5	-	-	4.8 ± 0.4	34.9 ± 1.1	13.7 ± 0.7	-
		25	-	-	3.4 ± 0.3	52.6 ± 2.7	6.5 ± 0.4	-
		32	-	-	0.2 ± 0.1	89.8 ± 3.9	0.2 ± 0.1	-

Table 2 cont.: Average (mean) \pm standard deviation of microbial metabolic activities during M156: bacterial carbon demand (BCD); bacterial growth efficiency (BGE); dissolved primary production

(PP_{DOC}); Percentage of extracellular release (PER); total primary production (PP_{TOT}) and the ratio between BCD and PPTOT ($\frac{BCD}{PP_{TOT}}$). BCD and BGE were obtained from BP and BR rates at 22°C (see text). ‘-’ indicate that the parameter was not measured and B.D. below detection (see text).

Location	Station	Depth (m)	BCD ($\mu\text{mol C L}^{-1} \text{d}^{-1}$)	BGE (%)	PP _{DOC} ($\mu\text{mol C L}^{-1} \text{d}^{-1}$)	PER (%)	PP _{TOT} ($\mu\text{mol C L}^{-1} \text{d}^{-1}$)	$\frac{BCD}{PP_{TOT}}$
Eddy Periphery	EDM-5E	All	-	-	-	-	-	-
	EDM-2E	All	-	-	-	-	-	-
	EDZ-4	All	-	-	-	-	-	-
	EDZ-3	All	-	-	-	-	-	-
	EDZ-2	5	10.5 ± 0.5	1.4 ± 2.2	2.9 ± 0.3	25.1 ± 3.4	11.9 ± 1.0	2.1
		15	9.4 ± 2.3	2.5 ± 0.7	4.9 ± 0.1	31.0 ± 1.7	14.5 ± 0.6	0.3
		50	B.D.	B.D.	-	-	-	-
		100	B.D.	B.D.	-	-	-	-
	EDZ-1	All	-	-	-	-	-	-
Frontal Zone	E3	5	7.1 ± 0.4	3.0 ± 1.7	7.8 ± 0.4	31.7 ± 1.7	25.0 ± 0.9	3.5 ± 2.2
		25	4.8 ± 1.1	2.8 ± 0.1	5.0 ± 0.6	33.4 ± 3.2	14.3 ± 0.8	3.0 ± 0.7
		45	1.9 ± 0.6	2.9 ± 2.1	0.7 ± 0.2	87.0 ± 3.3	0.8 ± 0.2	0.4 ± 0.3
		90	B.D.	B.D.	-	-	-	-
Open ocean	S4	All	-	-	-	-	-	-
	S3	5	3.2 ± 0.5	1.6 ± 0.2	1.3 ± 0.2	49.1 ± 5.5	2.7 ± 0.3	0.9 ± 0.5
		25	2.6 ± 0.5	1.7 ± 1.1	1.16 ± 0.03	38.4 ± 0.9	2.5 ± 0.03	1.0 ± 0.3
		50	1.2 ± 1.1	1.8 ± 0.2	0.0 ± 0.01	21.8 ± 6.6	0.1 ± 0.01	0.1 ± 0.1
		100	B.D.	B.D.	-	-	-	-
	E2	5	1.8 ± 0.6	1.8 ± 0.2	0.6 ± 0.1	40.9 ± 3.4	1.38 ± 0.1	0.8 ± 0.1
		25	3.5 ± 1.1	0.9 ± 0.04	0.94 ± 0.1	50.2 ± 3.1	1.89 ± 0.1	0.5 ± 0.1
		50	1.7 ± 0.4	1.6 ± 0.4	1.25 ± 0.3	91.3 ± 2.5	1.4 ± 0.3	0.8 ± 0.8
		100	B.D.	B.D.	-	-	-	-
	S2	All	-	-	-	-	-	-
	S1	All	-	-	-	-	-	-
	E1	5	0.4 ± 0.2	2.3 ± 0.02	0.23 ± 0.1	54.7 ± 13.3	0.39 ± 0.1	0.9 ± 0.5
		25	B.D.	B.D.	0.18 ± 0.01	38.5 ± 0.6	0.43 ± 0.01	-
		75	B.D.	B.D.	0.08 ± 0.02	61.7 ± 6.2	0.13 ± 0.02	-
		125	B.D.	B.D.	-	-	-	-

Location	Station	Depth (m)	BCD ($\mu\text{mol C L}^{-1} \text{d}^{-1}$)	BGE (%)	CR ($\mu\text{mol C L}^{-1} \text{d}^{-1}$)	PP _{DOC} ($\mu\text{mol CL}^{-1} \text{d}^{-1}$)	PER (%)	PP _{TOT} ($\mu\text{mol C L}^{-1} \text{d}^{-1}$)	PP _{DOC} / BCD (%)	PP / CR
Coastal	E5	5	0.6 ± 0.1	9.6 ± 3.7	1.7 ± 0.5	1.5 ± 0.2	34.9 ± 1.1	2.7 ± 0.2	217.4	1.6 ± 0.4
		20	0.5 ± 0.1	12.2 ± 2.6	1.3 ± 0.4	1.2 ± 0.1	52.6 ± 2.7	2.5 ± 0.1	231.4	1.9 ± 0.4
		35	0.5 ± 0.3	14.1 ± 1.7	1.3 ± 0.9	0.7 ± 0.1	89.8 ± 3.9	1.0 ± 0.1	143.2	0.71 ± 0.1
Eddy Periphery	EDZ-10N S6	All	-	-	-	-	-	-	-	-
		All	-	-	-	-	-	-	-	-
		All	-	-	-	-	-	-	-	-
Eddy Core	EDZ-8N	All	-	-	-	-	-	-	-	-
		All	-	-	-	-	-	-	-	-
		All	-	-	-	-	-	-	-	-
Eddy Core	EDZ-7N	5	3.6 ± 0.8	6.6 ± 0.5	7.3 ± 1.9	-	-	-	-	-
		20	3.6 ± 0.3	6.2 ± 2.6	7.3 ± 0.9	-	-	-	-	-
		All	-	-	-	-	-	-	-	-
Eddy Core	EDZ-6N	All	-	-	-	-	-	-	-	-
		All	-	-	-	-	-	-	-	-
		All	-	-	-	-	-	-	-	-
Eddy Core	EDZ-5N	5	2.8 ± 0.4	10.9 ± 2.5	5.6 ± 1.1	-	-	-	-	-
		20	1.2 ± 0.4	16.7 ± 3.7	2.8 ± 1.1	-	-	-	-	-
		30	0.4 ± 0.6	12.7 ± 0.5	1.2 ± 1.7	-	-	-	-	-
Eddy Core	EDM-4E	100	B.D.	B.D.	-	-	-	-	-	-
		5	4.7 ± 0.5	7.5 ± 1.9	8.9 ± 1.3	4.3 ± 0.1	36.7 ± 0.2	11.2 ± 0.1	87.9	1.3 ± 0.1
		15	1.4 ± 0.4	18.3 ± 1.0	3.1 ± 1.3	0.4 ± 0.1	39.3 ± 6.8	1.1 ± 0.1	29.5	0.3 ± 0.1
Eddy Core	EDM-3E	35	B.D.	B.D.	-	0.6 ± 0.3	94.4 ± 0.9	0.6 ± 0.3	-	-
		60	B.D.	B.D.	-	-	-	-	-	-
		All	-	-	-	-	-	-	-	-
Eddy Core	EDM-4	5	4.8 ± 1.1	5.9 ± 2.7	9.3 ± 2.9	4.3 ± 1.0	35.1 ± 5.7	12.6 ± 1.2	92.3	1.4 ± 0.4
		23	3.6 ± 0.2	8.1 ± 3.5	7.1 ± 0.7	3.9 ± 0.2	35.7 ± 1.4	11.0 ± 0.3	110.0	1.5 ± 0.4
		40	B.D.	B.D.	-	0.3 ± 0.1	85.3 ± 7.1	0.3 ± 0.1	-	-
Eddy Periphery	EDM-6E	100	B.D.	B.D.	-	-	-	-	-	-
		5	-	-	-	4.8 ± 0.4	34.9 ± 1.1	13.7 ± 0.7	-	-
		25	-	-	-	3.4 ± 0.3	52.6 ± 2.7	6.5 ± 0.4	-	-
Eddy Periphery	EDM-5E	32	-	-	-	0.2 ± 0.1	89.8 ± 3.9	0.2 ± 0.1	-	-
		All	-	-	-	-	-	-	-	-
		All	-	-	-	-	-	-	-	-
Eddy Periphery	EDZ-4	All	-	-	-	-	-	-	-	-
		All	-	-	-	-	-	-	-	-
		All	-	-	-	-	-	-	-	-

598

599

Table 2 continued:

Location	Station	Depth (m)	BCD ($\mu\text{mol C L}^{-1} \text{d}^{-1}$)	BGE (%)	CR ($\mu\text{mol C L}^{-1} \text{d}^{-1}$)	PP _{DOC} ($\mu\text{mol C L}^{-1} \text{d}^{-1}$)	PER (%)	PP _{TOT} ($\mu\text{mol C L}^{-1} \text{d}^{-1}$)	$\frac{PP_{DOC}}{BCD}$ (%)	$\frac{PP}{CR}$		
Eddy Periphery	EDZ-2	5	10.6 ± 0.7	2.7 ± 2.9	18.2 ± 1.4	2.9 ± 0.3	25.1 ± 3.4	11.9 ± 1.0	27.9	0.7 ± 0.7		
		15	9.6 ± 2.5	4.6 ± 1.3	16.5 ± 5.3	4.9 ± 0.1	31.0 ± 1.7	14.5 ± 0.6	46.8	0.9 ± 0.1		
		50	B.D.	B.D.		0	-	-0		-		
		100	B.D.	B.D.		-	-	-		-		
	EDZ-1	All	-	-		-	-	-		-		
		Frontal Zone	E3	5	7.3 ± 0.5	5.5 ± 2.4	13.1 ± 1.3	7.8 ± 0.4	31.7 ± 1.7	25.0 ± 0.9	108.1	1.9 ± 0.7
				25	5.0 ± 1.2	5.1 ± 0.2	9.5 ± 2.9	5.0 ± 0.6	33.4 ± 3.2	14.3 ± 0.8	96.3	1.5 ± 0.3
				45	1.9 ± 0.7	5.4 ± 4.0	4.4 ± 1.8	0.7 ± 0.2	87.0 ± 3.3	0.8 ± 0.2	37.8	0.2 ± 0.1
90	B.D.			B.D.		-	-	-		-		
Open ocean	S4	All	-	-		-	-	-		-		
		S3	5	3.2 ± 0.6	3.0 ± 0.4	6.9 ± 1.6	1.3 ± 0.2	49.1 ± 5.5	2.7 ± 0.3	41.4	0.4 ± 0.2	
	25		2.6 ± 0.5	3.1 ± 2.1	5.7 ± 1.5	1.16 ± 0.03	38.4 ± 0.9	2.5 ± 0.03	36.8	0.4 ± 0.1		
	E2	50	1.2 ± 1.1	3.3 ± 0.3	3.0 ± 2.9	0.0 ± 0.01	21.8 ± 6.6	0.1 ± 0.01	2.6	0.0 ± 0.01		
		100	B.D.	B.D.		-	-	-		-		
		5	1.8 ± 0.6	3.4 ± 0.4	4.3 ± 1.7	0.6 ± 0.1	40.9 ± 3.4	1.38 ± 0.1	31.4	0.3 ± 0.1		
		25	3.5 ± 1.1	1.7 ± 0.1	7.4 ± 2.9	0.94 ± 0.1	50.2 ± 3.1	1.89 ± 0.1	27.1	0.3 ± 0.1		
	50	1.7 ± 0.4	2.9 ± 0.8	4.2 ± 1.2	1.25 ± 0.3	91.3 ± 2.5	1.4 ± 0.3	72.6	0.3 ± 0.3			
	100	B.D.	B.D.		-	-	-		-			
	S2	All	-	-		-	-	-		-		
	S1	All	-	-		-	-	-		-		
		E1	5	0.4 ± 0.3	4.2 ± 0.04	1.3 ± 0.9	0.23 ± 0.1	54.7 ± 13.3	0.39 ± 0.1	52.4	0.3 ± 0.1	
25			B.D.	B.D.		0.18 ± 0.01	38.5 ± 0.6	0.43 ± 0.01		-		
75			B.D.	B.D.		0.08 ± 0.02	61.7 ± 6.2	0.13 ± 0.02		-		
125			B.D.	B.D.		-	-	-		-		

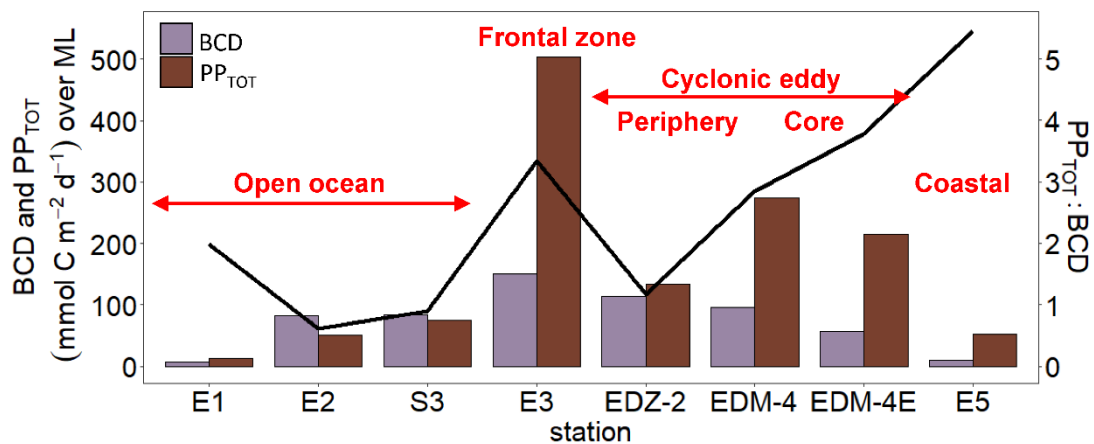
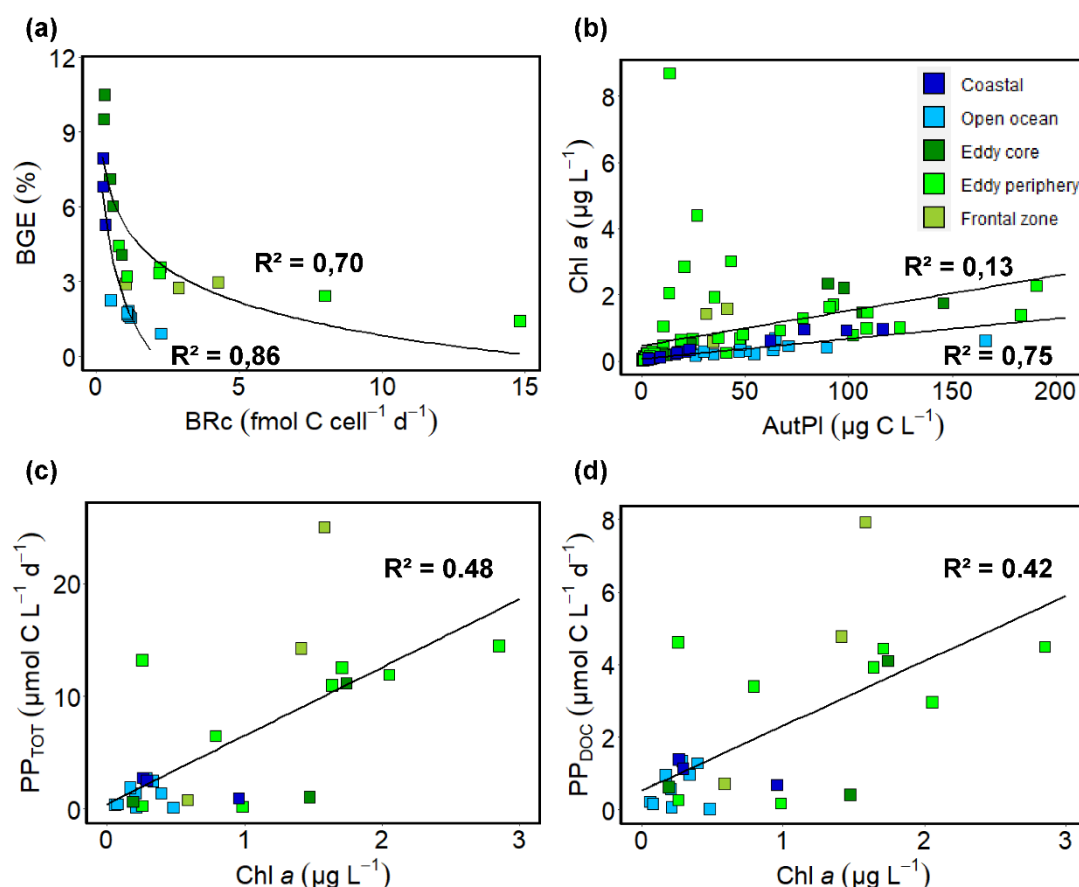


Figure 5: Integrated total primary production (PP_{TOT}) and bacterial carbon demand (BCD) rates over the mixed layer during M156. Blackline reports the ratio between PP_{TOT} and BCD. More information are given in SI table 1.

3.4 Indices of phyto- and bacterioplankton activity change

We investigated the impact of the CE on heterotrophic bacterial and phytoplankton abundance by regression analysis of cell-specific BR and BGE (Fig. 6a), as well as autotrophic plankton biomass and Chl *a* (Fig. 6b). We noticed a negative semilogarithmic relationship (Fig. 6a) between cell-specific BR rates and the BGE in both the zonal transect (coastal+open ocean) [$BGE = -3.11 \ln(\text{cell-specific BR}) + 2.35$; $R^2 = 0.86$; $p < 0.001$] and the eddy influenced region (CE + Frontal Zone) [$BGE = -1.92 \ln(\text{cell-specific BR}) + 5.28$; $R^2 = 0.70$; $p = 0.001$]. Concerning the phytoplankton (Fig. 6b), we observed that Chl *a* and autotrophic plankton biomass were linearly correlated in the open-ocean and coastal region ($R^2 = 0.75$; $p < 0.001$) while being poorly correlated in the CE-influenced area ($R^2 = 0.13$).



~~Figure 6: Relationship between (a) cell-specific bacterial respiration (BRe) and bacterial growth efficiency (BGE), (b) chlorophyll *a* (Chl *a*) and autotrophic plankton biomass (AutPI), (c) total primary production (PP_{TOT}) and Chl *a* and (d) dissolved primary production (PP_{DOC}) and Chl *a*. Black lines in (a) and (b) show regression from the open ocean and coastal stations (blue shades) and from the stations in eddy-influenced area (green shades). Black lines in (c) and (d) show regressions in all the stations.~~

3.5 Semi-labile dissolved organic carbon

Between coastal and open ocean stations, SL-DOC concentration was not significantly different (Tukey, $p > 0.05$; SI Fig. ~~S5b~~S4b) with ranges of $1.9\text{--}8.0\text{ }\mu\text{mol L}^{-1}$ at the coastal and $4.7\text{--}18.9\text{ }\mu\text{mol L}^{-1}$, respectively at the open ocean stations. At those sites, SL-DOC distribution was rather uniform in the upper 40 m with SL-DOC $> 5\text{ }\mu\text{mol L}^{-1}$, apart except from the station furthest offshore from $22.7\text{--}24.3^{\circ}\text{W}$ (St. E1) where SL-DOC $> 5\text{ }\mu\text{mol L}^{-1}$ was limited to shallow depth depths (5 m). In the CE and at the Frontal Zone, SL-DOC concentration was clearly elevated and increased from East east to West west with an overall range of $1.4\text{--}54.34\text{ }\mu\text{mol L}^{-1}$. At the Frontal Zone, SL-DOC concentration $> 5\text{ }\mu\text{mol L}^{-1}$ was detectable down to 90 m depth.

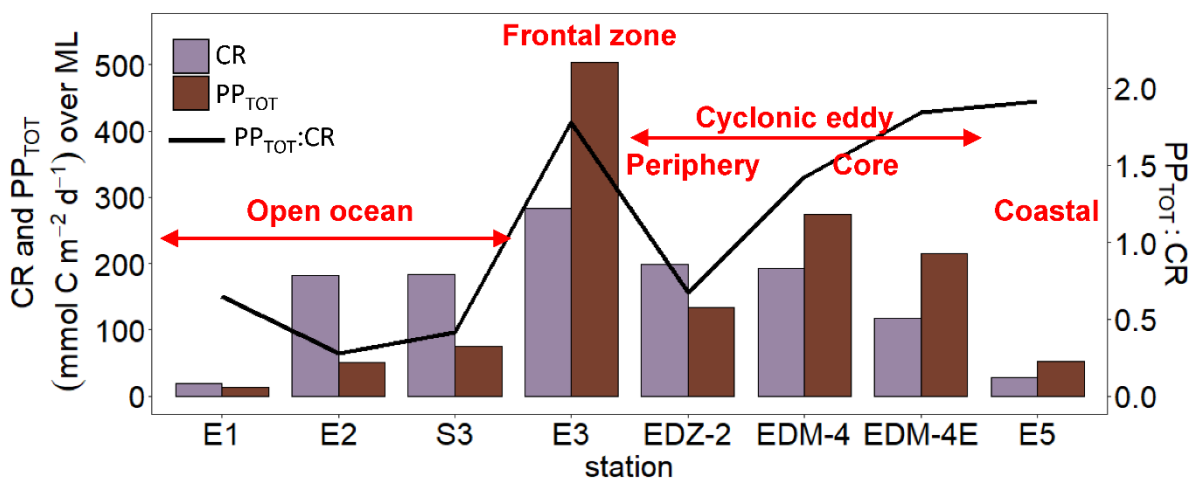


Figure 6: Integrated total primary production (PP_{TOT}) and community respiration (CR) rates over the mixed layer during M156.

3.6 Correlation analysis

We applied a Pearson correlation matrix (Fig. 7) to reveal significant correlations between the measured parameters. Temperature in the stations outside (open ocean + coastal) and inside

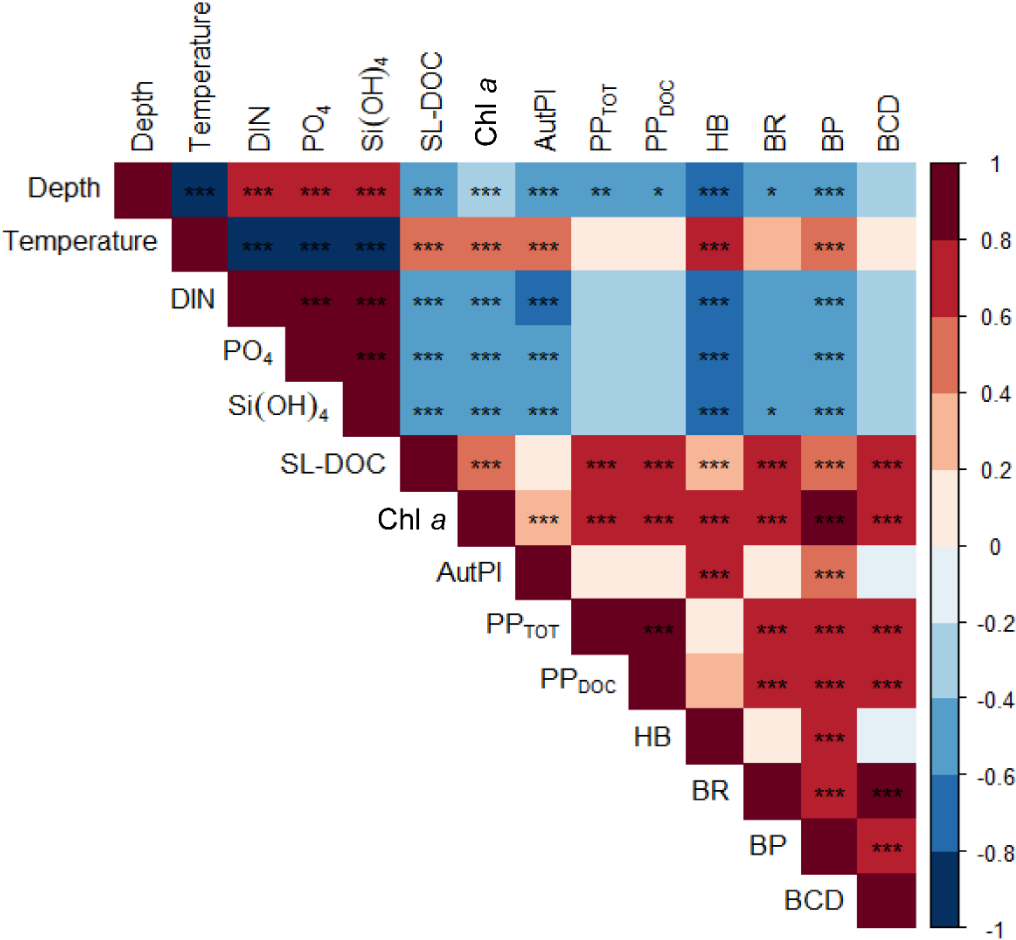
(cyclonic eddy + frontal zone) the area influenced by the eddy. In both regimes, temperature correlated negatively with nutrients (DIN, PO₄, Si(OH)₄; ~~Pearson, R=-0.9~~ $r = -0.70, -0.67$ and -0.67 respectively for the stations outside and $r = -0.97, -0.96$ and -0.95 for the stations inside the area influenced by the eddy, $p < 0.001$) and positively with ~~bacteria~~ (Pearson, R=~~bacterial~~ abundances ($r = 0.6551$ and 0.68 respectively, $p < 0.001$). ~~Total~~

In the stations outside the influence of the eddy, total (PP_{TOT}) and dissolved primary production (PP_{DOC}) ~~rates~~ were ~~positively~~~~not~~ correlated to ~~each other~~ (Pearson, R=~~0.98~~, $p < 0.001$) and to Chl-*a* and SL-DOC (Pearson, R=~~0.65~~ and ~~0.60~~ respectively, $p < 0.001$), but not to the autotrophic ~~plankton~~~~pico- and nanoplankton~~ biomass (Pearson, R=~~0.14~~, $p > 0.05$). ~~Bacterial~~In contrast, heterotrophic bacterial abundance (HB) and the bacterial biomass production (BP) and respiration (BR) were ~~positively~~ correlated (Pearson, R=~~to primary productivity rates~~ ($r = 0.78$, $p < 0.001$). BCD was more correlated to BR than to BP (Pearson, R=~~1~~ and ~~0.74~~ respectively, $p < 0.001$). A clear coupling between phytoplankton and bacteria was indicated, by positive correlations between PP_{TOT} and PP_{DOC} and BP, BR, ~~85~~ and BCD (Pearson, R=~~0.70~~, $p < 0.001$), BP~~82~~ respectively for PP_{TOT} and Chl-*a* (Pearson, R=~~0.77~~ and ~~0.9377~~ respectively for PP_{DOC}, $p < 0.001$), and BRChl-*a* ($r = 0.64$ and ~~Chl-*a*0.72~~ respectively, $p < 0.001$) and autotrophic pico- and nanoplankton biomass, ($r = 0.42$ and 0.46 respectively, $p < 0.001$) and the SL-DOC concentration (Pearson, R=~~of semi-labile DOC (SL-DOC; $r = 0.7861$ and 0.7556 , $p < 0.001$). However, bacterial respiration (BR), was not correlated to any variable ($p > 0.05$).~~

In the stations influenced by the eddy, PP_{TOT} was positively correlated to Chl-*a* ($r = 0.55$, $p < 0.05$) whereas PP_{DOC} ($r = 0.47$, $p > 0.05$) was not, and both were not correlated to the autotrophic pico- and nanoplankton biomass. Chl-*a* and SL-DOC were significantly correlated ($r = 0.36$, $p < 0.001$). Heterotrophic bacterial and autotrophic pico- and nanoplankton abundance and activities were coupled but differently than in the stations outside the eddy. HB was not correlated to PP_{TOT} and PP_{DOC} ($p > 0.05$), but was strongly correlated to Chl-*a* and autotrophic pico- and nanoplankton biomass ($r = 0.57$ and 0.76 , respectively, $p < 0.001$) but not to SL-DOC ($r = 0.19$, $p > 0.05$). BP, on the contrary, was correlated to PP_{TOT} and PP_{DOC} ($r = 0.63$ and 0.59 , respectively, $p < 0.05$) and strongly to Chl-*a* ($r = 0.92$, $p < 0.001$). BP correlated also to autotrophic pico- and nanoplankton biomass and to SL-DOC, albeit to a lesser extent ($r = 0.41$ and 0.43 , respectively, $p < 0.05$). In contrast to stations not influenced by the eddy, BR was strongly correlated to Chl-*a* and SL-DOC ($r = 0.83$ and 0.76 , respectively, $p < 0.001$). However, BR was not significantly correlated to autotrophic pico- and nanoplankton biomass, PP_{TOT}, and PP_{DOC} ($r = -0.05, 0.61$ and 0.50 respectively, $p > 0.05$).

678

679



680

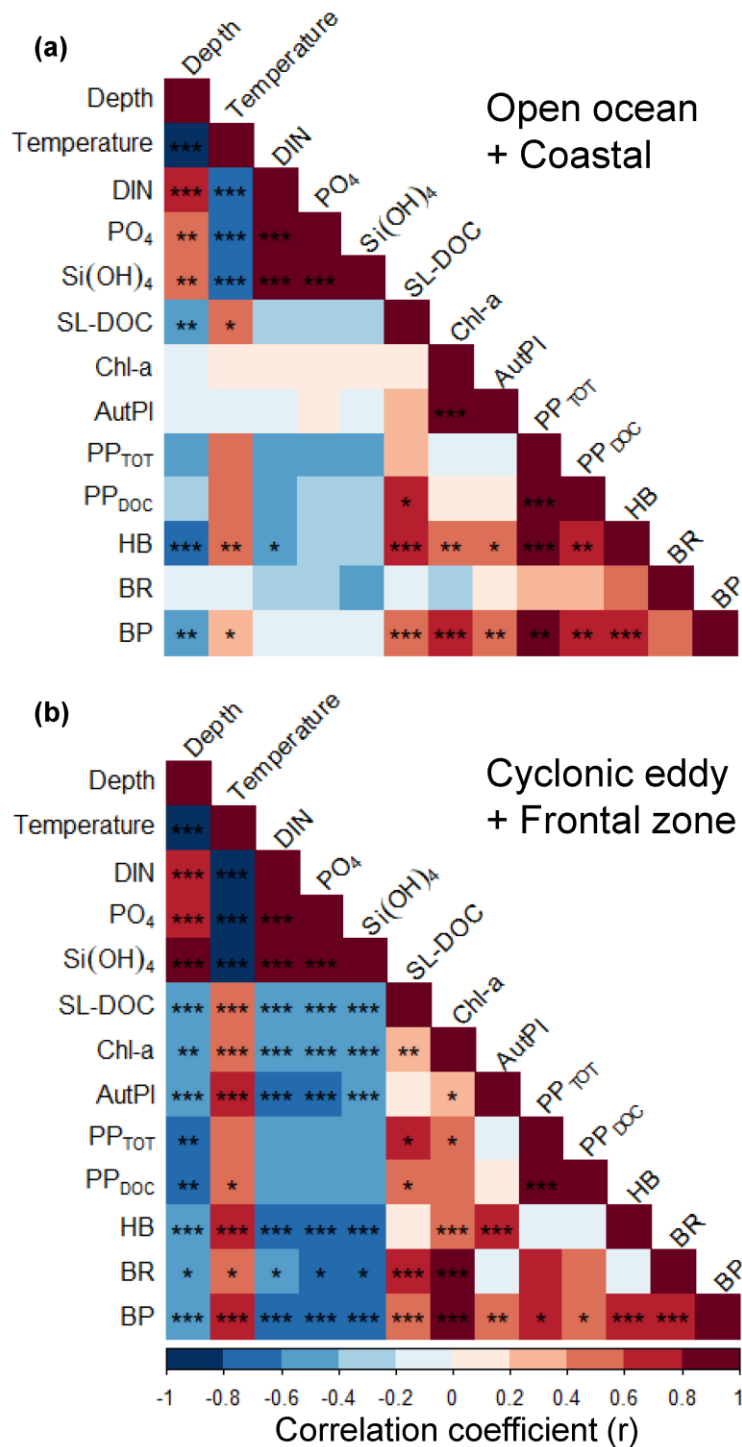


Figure 7: Pearson correlation matrix of biochemical parameters, metabolic activities, and bacterial abundance in the upper 200 m during M156. Colour scale: correlation coefficient (r) in samples not influenced by the cyclonic eddy (i.e., coastal and open ocean stations) (a) and samples influenced by the cyclonic eddy (b). Statistical significance: '***' < 0.001, '**' < 0.01, '*' < 0.05.

4. Discussion

4.1 ~~Distribution~~ Effect of a cyclonic eddy on the distribution of phytoplankton abundance and activity in the Mauritanian upwelling system ~~associated with cyclonic eddy perturbation~~

In general, coastal Chl-*a* concentration during this study was not as high as observed in earlier studies with strong coastal upwelling (e.g., Alonso-Sáez et al., 2007; Agustí and Duarte, 2013; Arístegui et al., 2020). This might be related to the relatively weak upwelling, ~~as a result of~~ resulting from weak surface winds along the Mauritanian Coast typically occurring during summer when our samples were collected (~~Peligrí~~Pelegrí and Peña-Izquierdo, ~~2015a~~2015). Consequently, during summer, fewer nutrients reach the euphotic zone ~~by coastal upwelling,~~ while. At the same time, offshore surface wind ~~remains~~remained strong ~~and might enhance,~~ enhanced vertical mixing ~~at the surface. Coastal and may explain why coastal~~ Chl-*a* concentration was only slightly higher compared to the open ocean, ~~and both. When excluding~~ the ~~coastal and open ocean phytoplankton communities were dominated by cells <20µm, as indicated by the strong linear correlation between Chl-*a* and autotrophic plankton biomass (Fig. 6b).~~

~~We did not observe eddy-influenced stations, there was no~~ marked gradient in phytoplankton productivity either, unlike other regions of the CanUS ~~with permanent upwelling conditions~~ (Demarcq and Somoue, 2015; Arístegui et al., 2020). PP_{TOT} and PP_{DOC} rates stayed rather constant from the coast to the open ocean and were in the range of reported rates in oligotrophic offshore waters of the CanUS (Agustí and Duarte, 2013; Lasternas et al., 2014). ~~SL-DOC was relatively constant as well, with variations attributable to the westward propagation of the currents and eddies (SI Fig. S5b; Lovecchio et al., 2017, 2018). The absence of upwelling and the dominance of small autotrophic cells (<20µm) in the phytoplankton community suggest that in the open ocean and coastal stations, primary productivity was maintained through remineralisation of nutrients released from dying cells. Indeed, plankton mortality rates have been reported to increase with decreasing cell size (Marbá et al., 2007) and with increasing PER (Lasternas et al., 2014). Spatial distribution of SL-DOC was relatively uniform as well when considering the coastal and open ocean stations only. PER in our study was on average 51.1 ± 17% in both the open ocean and the coastal stations, which contrasts previous findings. For example, Agustí and Duarte (2013) reported PER to range from ~1% in ‘healthy’ communities from the upwelled waters of the CanUS to ~70% in ‘dying’ communities from the oligotrophic~~

waters of the ETNA. ~~PER in our study was on average $51.1 \pm 17\%$ in the open ocean and coastal stations leading to the conclusion that primary productivity in those areas was maintained mainly through remineralisation of small ($<20\mu\text{m}$) plankton cells~~PER have been reported to increase with nutrient depletion (Obenosterer and Herndl, 1995; Agustí and Duarte, 2013; Lasternas et al., 2014; Piontek et al., 2019) among other factors (see review by Mühlenbruch et al., 2018). Since upwelling was weak during our sampling period, low nutrient concentrations in the surface waters might explain the relatively high PER that we observed near the coast.

The CE broke this rather uniform distribution of phytoplankton productivity ~~and community through from the~~ coastal ~~and to the~~ open ocean waters. ~~From a depth distribution perspective,~~ Chl-*a* isolines ~~seemed to have been~~ were pushed ~~toward~~towards the surface in the CE (Fig. ~~3a4a~~). Similar ~~‘compression’~~uplifting of Chl-*a* isolines towards the surface ~~have~~has been reported ~~in for other~~ eddies ~~earlier~~ (Lochte and Pfannkuche, 1987; Feng et al., 2007; Noyon et al., 2019). ~~Such compressions have been attributed to resulting) and might result~~ from phytoplankton ~~growth~~relocation through ~~upwelling of nutrients combined with high~~intense vertical mixing ~~from by~~ strong surface winds, ~~which favour phytoplankton distribution at the surface~~ (Feng et al., 2007; Noyon et al., 2019). ~~In the CE, the upwelling was marked by the hydrographic parameters (e.g. temperature, salinity, nutrients, Fig. 2), and before the~~Before our eddy survey, strong surface winds occurred offshore (SI Fig. ~~S7~~). ~~Therefore, the phytoplankton which grew from upwelled nutrients must have been relocated to the surface through mixing, the reason why S5), which might explain the~~ high Chl-*a* concentration ($>0.5 \mu\text{g L}^{-1}$) ~~concentration was that we~~ found at the surface (~~5m~~in 5 m) of all stations within the CE.

~~In addition, Chl-*a* was dispatched differently within the CE with the highest concentrations in the Western and Northern part and lowest concentrations in the Southern and Eastern part (Table 1; SI Fig. S4). Furthermore, an almost continuous deepening of high Chl-*a* ($>0.5 \mu\text{g L}^{-1}$) distribution, as well as an increase of SL-DOC concentration, was~~Within the eddy, we observed that Chl-*a* was higher in the CE ~~from East to West~~western than in the eastern part of the eddy (Fig. ~~3a; SI Fig. S5b3b and 4a~~). Chelton et al. (2011) ~~established from~~showed based on satellite observation ~~and an eddy-centric perspective~~ that due to the rotational flow and the westward propagation of CEs, Chl-*a* tends to accumulate in their ~~Southwest~~southwest quadrants while being lower in their ~~Northeast~~northeast quadrants. ~~Since in our case, the CE shape was elliptic, we assume that the rotational flow in the CE changed, shifting the accumulation.~~To the best of our knowledge, this is the first time that high-resolution in situ sampling could demonstrate this specific submesoscale Chl-*a* distribution within a CE.

Outside of the CE boundaries, we noticed a thermal front with colder surface water. Thermal fronts ~~are often have been~~ detected ~~out outside of the periphery~~ of eddies ~~periphery as a consequence of and interpreted to result from~~ eddy-eddy interaction (See review by Mahadevan, 2016) and/or eddy-wind interaction (Xu et al., 2019). In this Frontal Zone, we observed higher nutrient ~~content concentrations~~ than ~~in~~ the adjacent stations ~~including the western part of the CE periphery~~ and a doming of the nutriclines ~~marking an, which indicates~~ upwelling (~~see Fig. 2a, d-f). Thus 2).~~ Consequently, Chl-*a* was elevated, and ‘compressed’ to the surface ~~in this area~~ similarly as in the CE (Fig. 3a). ~~We assume this distribution to be the consequence of the same factors affecting the CE (upwelling, mixing induced by strong surface winds). 4a).~~

~~In the CE-influenced area (CE+Frontal Zone), Chl-*a* concentration was disconnected from small (<20µm) autotrophic plankton biomass (Fig. 6b). This implies that in the West of the eddy where Chl-*a* was high and small autotrophic plankton biomass low (Fig. 3a & b), larger autotrophic cells such as diatoms and/or dinoflagellate were present in higher quantities. We corroborate this point from lipid biomarkers concentration (unpublished Our flow cytometry data) as fucoxanthin, a typical marker of diatoms (Stauber and Jeffrey, 1998), was the dominant pigment in the Western part of the CE. This is consistent with previous studies in which CEs unevenly altered the phytoplankton community, often reporting the presence of diatoms/dinoflagellates (e.g., (SI Fig. S6) showed that Lochte and Pfannkuche, 1987; Lasternas et al., 2013). The details of autotrophic plankton composition (SI Fig. S7) confirm this diversity, with the uneven distribution of cyanobacteria (*Synechococcus*) and eukaryotic pico- and nanoplankton within the CE underseoring the fact were unevenly distributed. This suggests that the phytoplankton community of the CE was likely separated distinct from the transect and diverse within a surrounding waters, but also variable on the submesoscale within the CE. This is consistent with previous studies on phytoplankton distributions in eddies (e.g., Lochte and Pfannkuche, 1987; Lasternas et al., range.~~

~~Therefore, the CE dispatched different phytoplankton taxa with different potentials of primary production and resources acquisition. 2013; Hernández-Hernández et al., 2020).~~ Moreover, the mixed layer was also highly variable within the CE ~~leading to substantial variation of and so were~~ PP_{TOT} rates (SI Table 1, Figure 5). Hence, we ~~SI, Figs. 3 and 6).~~ We observed a three-fold variation of depth-integrated PP_{TOT} rates over 100m depth (Table 1) within the CE which is coherent with earlier observations of a ~~fivefold five-fold~~ variation of primary production integrated over the euphotic zone in a CE in the subtropical Pacific Ocean (Falkowski et al., 1991). Overall, primary productivity was enhanced within the CE and the Frontal Zone with an

average of ~~fourfold~~four-fold more depth-integrated PP_{TOT} rates over ~~100m~~100 m depth than in the open ocean and coastal stations. This is coherent with Löscher et al. (2015)), who found that depth-integrated primary productivity over the ~~ehlorophyll~~Chl-*a* maximum of a CE in the Mauritanian upwelling system was ~~threefold~~three-fold higher than in the surrounding waters. ~~Exudation~~Extracellular release rates (PP_{DOC}) were also enhanced within the eddy ~~and integrated~~ ~~(0-100 m) PP_{DOC} rates were on average three-fold time higher than in the transect (Table 1).~~ ~~Yet, even if PP_{DOC} rates were higher within the CE and at the Frontal Zone stations (Table 2),~~ but PER was slightly lower at the eddy surface (Fig. ~~3d4d~~4d, e). We ~~start from~~emit two hypotheses regarding this distribution: 1) the lower PER ~~reported~~ was due to a higher proportion of larger phytoplankton (e.g., diatoms) ~~who~~, which have lower turnover rates and therefore ~~have~~ lower PER and/or 2) the upwelling of nutrients generated by the CE might have enhanced the physiological health of the phytoplankton community ~~(Agustí and Duarte, 2013; Laternas and Agustí, 2014).~~

4.2 ~~Heterotrophic bacteria~~Variations in heterotrophic bacterial abundance and ~~activities~~ responses in the Mauritanian upwelling systemactivity associated with a cyclonic eddy

Along the zonal transect, in the stations not affected by the eddy (open ocean+coastal stations), a ~~strong coupling~~significant positive correlation was observed between HB abundance and PP_{TOT} rates ~~was observed (R²=0.72).~~ Therefore, HB ~~abundance followed the same trends as the PP_{TOT} by being continuously~~(Fig. 7a). Those variables were rather uniformly distributed from the coast to the offshore waters: excluding samples influenced by the eddy, which is in agreement with earlier findings by Bachmann et al. (2018) ~~reported a similar trend in~~for the Mauritanian upwelling system during summer, ~~strengthening our finding.~~

~~Bacterial activities were distributed differently.~~ Both our BR and BP were also within the range of reported rates for coastal and offshore ~~water~~waters of the CanUS (Reinthal et al., 2006; Alonso-Saez et al., 2007; Vaqué et al., 2014). BP rates slightly decreased from the coast to the open ocean: when samples from the eddy were not considered. Similar trends were found in the CanUS with different upwelling intensities and atduring different seasons (Alonso-Saez et al., 2007; Vaqué et al., 2014). ~~Therefore, those factors (upwelling intensity and seasonality) were likely only indirectly coupled with BP variability, which instead was rather driven by the composition of the phytoplankton community. Indeed, BP was more correlated to Chl-*a* than~~

autotrophic plankton biomass ($<20\mu\text{m}$; Fig. 7) suggesting that BP was more enhanced by the presence of larger autotrophic cells, such as diatoms or dinoflagellates. Those have larger phycospheres allowing them to attract more bacteria by chemotaxis (see review by Seymour et al., 2017). Hence, bacteria may benefit from mutualistic relationships with larger algae increasing their BP. Fucoxanthin, was decreasing from the coastal to offshore waters with overall low relative abundance (5-15%) (data not shown). Being part of microphytoplankton, especially diatoms have higher viability in coastal than in offshore waters of the CanUS (Lasternas et al., 2013), which may explain the observed fucoxanthin gradient.

In contrast, BR rates were higher in offshore than in coastal waters. BR rates were coupled to SL-DOC concentration, which is in agreement with Xu et al. (2013), who also found BR to be enhanced by low molecular weight DOC compound ($<30\text{kDa}$). SL-DOC compounds have a turnover of weeks to months, which allows them to escape rapid microbial degradation (Hansell et al., 2009). In the CanUS, currents and eddies can laterally transport DOC up to 2000 km (Lovecchio et al., 2018). Hence, we state that SL-DOC compounds produced at the coast have been relocated offshore while being slowly respired by heterotrophic bacteria along the way.

The distinct distribution of BP and BR rates affected the distribution of the BGE, which was higher in the coastal than in the open ocean stations. This is in accordance with observations by Overall, our BGEs represent the lower end of global ocean values, but similarly low BGEs have been observed for other EBUS, such as the CanUS (Alonso-Sáez et al., 2007) who showed higher BGE in the upwelling area above Cape Blanc than in the offshore waters of the CanUS. Overall, the BGEs reported here are among the lowest reported with all values $<11\%$, but not surprising since BGE is negatively correlated to temperature and, therefore, reduced in the tropical ocean (Rivkin and Legendre, 2001). Yet we the California upwelling system (del Giorgio et al., 2011) and the Humboldt upwelling system (Maßmig et al., 2020). Yet, we report an average BGE threetwo times lower than Alonso-Sáez et al., (2007). We assume this difference), which may be due to result from the difference differences in upwelling intensity (none vs. permanent). Indeed, Kim et al. (2017) denoted that BGE increased with increasing upwelling intensity in the Ulleung Basin. Under none or low upwelling conditions, bacteria compete with At the coast, PP_{DOC} rates were sufficient to compensate for the BCD, indicating a strong trophic dependence of bacteria on phytoplankton, whereas in the open ocean PP_{DOC} rates covered up between 2.6 to 78% indicating a much lower trophic dependence of bacteria on phytoplankton. Therefore, in the open ocean, other carbon sources (i.e., PP_{POC} , SL-DOC) must have been used to compensate the BCD. SL-DOC compounds have a turnover of weeks to

months, which allows them to escape rapid microbial degradation (Hansell et al., 2009). Consequently, we hypothesize that the BCD in the open ocean was sustained through SL-DOC produced in excess near the coast and transported offshore. Indeed, in the CanUS, currents and eddies have been shown to laterally transport DOC offshore up to 2000 km (Lovecchio et al., 2018). ~~for nutrient acquisition. Moreover, as microphytoplankton do not thrive in the water column due to their high nutrient requirements (see review by Marañón, 2015), bacteria benefit less from their phycospheres. Hence, we expect BP to be lower in the relaxation period (May to July) post upwelling than in the upwelling season (January to March; Lathuilière et al., 2008) in the Mauritanian upwelling system.~~

Within the CE-influenced stations (CE + Frontal Zone), HB abundance was disconnected from the PP_{TOT} rates (Fig. 4a). ~~HB abundance was significantly higher in the core of eddy but surprisingly low at the Southwestern side of the eddy 7b). For example, in the southwestern periphery (18.83 to 19.11 °W), where and the frontal zone HB abundances were relatively low, while both PP_{TOT} rates and Chl-*a* concentrations were relatively high (Fig. 3a4a, c). Hernández et al. (2020) reported a similar feature observation with a strong disparity heterogeneity of HB biomass distribution within a CE in the CanUS. Since Chl-*a* and SL-DOC compounds accumulated in the Southwestern part of the CE, gel-like Attachment to particles produced, viral lysis or grazing by phytoplankton and bacteria such as transparent exopolymer particles (TEP) (Passow, 2002) nanoflagellates might have also accumulated there. We hypothesize that a missing fraction of led to a selective reduction in HB abundance. However, the exact reasons for the low HB occurrence at the eddy periphery and the bacteria might have been attached to gel-like particles (Busch et al., 2018) or other particulate matter.~~

~~The~~ Frontal Zone are unknown. Despite the low HB abundance, BP was particularly stimulated within the CE in these areas. On average, BP was three-fold higher in the eddy influenced stations and on average threefold higher than in compared to the open ocean stations ones when integrated over 100 m. This is in accordance with earlier studies from the Sargasso Sea (Ewart et al., 2008), the CanUS (Baltar et al., 2010), and in the Mediterranean Sea (Belkin et al., 2022), where CEs enhanced BP has been observed in CE. As stated previously, the upwelling induced by the CE and the Frontal Zone led to higher phytoplankton biomass, including diatoms and/or dinoflagellates which were likely responsible for this increase in BP, which was likely responsible for this overall increase in BP. However, it is noteworthy that BP and PP_{TOT} rates were less correlated than in the zonal transect. BR rates were also enhanced at the surface of the CE and followed a similar trend as BP. SL-DOC concentrations showed a strong positive

correlation with BR, which makes sense considering that high molecular weight DOC compounds (>1 kDa) are a favourable carbon source for heterotrophic microbes (Amon and Benner, 1994, 1996; Benner and Amon, 2015). PP_{DOC} rates in the CE covered 27.9% to 110% of the BCD, indicating a moderate to strong trophic dependence of bacteria on phytoplankton in CE. Although PP_{TOT} globally may satisfy the BCD in the CE (43.1-341%) a question remains about why BGE was low in the CE (2.7-18.3%).

~~BR rates were also enhanced at the surface of the CE and were coupled to the SL-DOC concentration. Since the CE was relatively young (1.5 months old), autochthonous SL-DOC compounds produced by exudation (PP_{DOC}) must have been merged with allochthonous coastal SL-DOC compounds transported during the CE formation. PP_{DOC} rates in the CE covered 28.3 to 114.5% of the BCD, indicating a moderate to strong trophic dependence of bacteria on phytoplankton in CE (Fouilland and Mostajir, 2010). Although PP_{TOT} may satisfy the BCD in the CE through the bacterial incorporation of phytoplankton-derived DOC from sloppy feeding, exudation, viral infection, or cell apoptosis, a question remains about why heterotrophs preferentially used SL-DOC compounds for respiration rather than for biomass production. We start from two hypotheses, firstly, the SL-DOM compounds had a high C/N ratio leading to an increase of BR and a decrease of BGE (Lønborg et al., 2011). Secondly, SL-DOC was easier to access for bacteria than other nutrients. Phytoplankton DOM exudate/lysates are more or less labile following their origin (e.g. diatoms/cyanobacteria) and are depleted in the nutrient (e.g. nitrate/phosphate) limiting phytoplankton growth (e.g. Pete et al., 2010; Wear et al., 2020). As the phytoplankton community was diverse within the CE and as the CE likely transported allochthonous DOM, a multitude of compounds with specific qualities coexisted in the CE. Therefore, bacteria may have used SL-DOC as fuel to degrade DOM compounds containing limiting nutrients for their growth (Guillemette et al., 2016).~~

~~The diversity of DOM from different origins (e.g. cyanobacteria/diatom) within the CE likely induced distinct bacterial communities. We noticed a negative semilogarithmic relationship (Fig 6) between cell-specific BR and the BGE in both the zonal transect (coastal+open ocean stations) and the CE influenced (CE + Frontal Zone) stations. The slopes of the curves and the ranges of cell-specific BR values were different between the two systems suggesting distinct bacterial communities with different degrees of resource optimization (Baña et al., 2014). Within the CE, the bacterial community was probably as the phytoplankton community even more diverse as observed in previous CEs studies (Zhang et al., 2011; Yan et al., 2018).~~

Our results show that bacteria do not grow proportionally to the amount of DOM they received through exudation but rather depends on the different requirement between respiration and biomass production. In response, the BGE varied sevenfold within the CE (1.4–10.5%) whereas it varied twofold in the open ocean (0.9–2.3%) and in the coastal (5.3–7.9%) stations. Robinson (2008) suggested that most of the BGE variability within oligotrophic waters is explained by BR. Here we hypothesise that in CEs, which cross oligotrophic waters in the ETNA, BGE variability depends on both BP through phytoplankton taxonomical composition and BR through the amount and quality of the SL-DOC.

Overall, we showed that autotrophy prevails in the upper ~~100m~~100 m depth of Mauritanian coastal waters while heterotrophy prevailed offshore. This is coherent with a modeling study from Lovecchio et al. (2017). The CE and the associated Frontal Zone fuelled phytoplankton ~~nutrients~~nutrient needs and maintained autotrophy further offshore. ~~The highest PP_{TOT} inside of the eddy and the most pronounced autotrophy were determined at~~especially in the Frontal Zone, where highest PP_{TOT} were measured. Mouriño-Carballido (2009) reported from indirect estimations of net community production that the frontal zones between CEs and ACEs are among the most productive ~~area~~areas in the North–West subtropical Atlantic Ocean. Previous studies ~~showed~~have shown that the trophic balance could switch from autotrophy to heterotrophy in an eddy within a month(s) (Maixandeu et al., ~~2003~~2005; Mouriño-Carballido ~~et al., and McGillicuddy~~, 2006). Here we ~~report with a small timescale (11 days) that in a CE, states of little to high~~showed that both autotrophy ~~occurred. Thus, phytoplankton dynamic and associated bacterial responses and heterotrophy can occur~~ within ~~eddies not only change with time but also through space~~a single eddy. This urges the need for more high-resolution eddy studies in order to better estimate their impact on plankton metabolic activities and carbon cycling.

Conclusion

Our results highlight the ability of a CE to be an autotrophic vector ~~towards~~toward the open ocean with organic matter freshly produced by the phytoplankton community inside. Yet, despite the strong autotrophy associated with the CE, phytoplankton exudation of DOM was not always enough to compensate for bacterial metabolic needs. Even if BP was enhanced in the CE, the BGE was rather low and varied substantially. ~~This implies that~~Instead, heterotrophic bacteria ~~recycle allochthonous~~preferentially used DOM ~~transported by the eddy and/or have~~

~~issues to degrade phytoplankton DOM for respiration.~~ Microbial metabolic ~~activities~~
~~dynamic~~activity dynamics within eddies are complex and require further investigations to better
understand and unravel ~~the~~ carbon cycling in these features.

Data availability

All data will be made available at the PANGEA database (data manager, webmaster: Hela Mehrstens)

Author contribution

QD, KWB and AE designed the scientific study, analyzed the data and wrote the paper. AB, did the eddy reconstruction and both ~~AE~~AB and JH commented on the paper.

Competing interests:

The authors declare that they have no conflict of interest.

Acknowledgments

We thank the captain and the crew of the *R/V Meteor* for their support during the M156 cruise. We thank J. Roa, T. Klüver and L. Scheidemann for sampling on board. We thank J. Roa and S. Golde additionally for the analysis of dissolved organic matter and T. Klüver for cell counting, bacterial and phytoplankton activities analyses. We thank B. Domeyer and R. Suhrberg for the nutrient analyses. This study has been conducted using E.U. Copernicus Marine Service Information. The results contain modified Copernicus Climate Change Service information 2020. Neither the European Commission nor ECMWF is responsible for any use that may be made of the Copernicus information or data it contains. This study is a contribution of the REEBUS project (Role of Eddies in the Carbon Pump of Eastern Boundary Upwelling Systems) sub-projects WP1 and WP4, funded by the BMBF (funding reference no. 03F0815A).

Reference

Agustí, S., and Duarte, C. M.: Phytoplankton lysis predicts dissolved organic carbon release in marine plankton communities, *Biogeosciences*, 10, 1259-1264, <https://doi.org/10.5194/bg-10-1259-2013>, 2013.

Alonso-Sáez, L., Gasol, J. M., Arístegui, J., Vilas, J. C., Vaqué, D., Duarte, C. M., and Agustí, S.: Large-scale variability in surface bacterial carbon demand and growth efficiency in the subtropical northeast Atlantic Ocean, *Limnol. Oceanogr.*, 52, 533-546, <https://doi.org/10.4319/lo.2007.52.2.0533>, <https://doi.org/10.4319/lo.2007.52.2.0533>, 2007.

Amon, R. M. W., and Benner, R.: Rapid cycling of high molecular weight dissolved organic matter in the ocean, *Nature* 369, 549–552. doi: 10.1038/369549a0, 1994.

Anderson, T. R., and Ducklow, H. W.: Microbial loop carbon cycling in ocean environments studied using a simple steady-state model, *Aquat. Microb. Ecol.*, 26, 37-49. 2001.

Aranguren-Gassis, M., Teira, E., Serret, P., Martínez-García, S., and Fernández, E.: Potential overestimation of bacterial respiration rates in oligotrophic plankton communities, *Mar. Ecol. Prog. Ser.*, 453, 1–10, <https://doi.org/10.3354/meps09707>, 2012.

Arístegui, J., Barton, E. D., Álvarez-Salgado, X. A., Santos, A. M. P., Figueiras, F. G., Kifani, S., Hernández-León, S., Mason, E., Machú, E., and Demarcq, H.: Sub-regional ecosystem variability in the Canary Current upwelling, *Prog. Oceanogr.*, 83, 33-48, <https://doi.org/10.1016/j.pocean.2009.07.031>, 2009.

Arístegui, J., Montero, M. F., Hernández-Hernández, N., Alonso-González, I. J., Baltar, F., Calleja, M. L., and Duarte, C. M.: Variability in Water-Column Respiration and Its Dependence on Organic Carbon Sources in the Canary Current Upwelling Region, *Front. Earth Sci.*, 8, 1-12. <https://doi.org/10.3389/feart.2020.00349/>, 2020.

Arístegui, J., Tett, P., Hernández-Guerra, A., Basterretxea, G., Montero, M. F., Wild, K., Sangrá, P., Hernández-León, S., Cantón, M., García-Braun, J. A., Pacheco, M., and Barton, E. D.: The influence of island-generated eddies on Chl a distribution: a study of mesoscale variation around Gran Canaria, *Deep-Sea Res.*, 44:71-96. 1997.

Armon, R. M. W., and Benner, R.: Bacterial utilization of different size classes of dissolved organic matter. *Limnol. Oceanogr.*, 41(1), 41–51, 1996.

Bachmann, J., Hassenrück, C., Gärdes, A., Iversen, M. H., Heimbach, T., Kopprio, G. A., and Grossart, H. P.: Environmental Drivers of Free-Living vs. Particle-Attached Bacterial Community Composition in the Mauritania Upwelling System. *Front. Microbiol.*, 9, 1–13, <https://doi.org/10.3389/fmicb.2018.02836>, 2018.

Baltar, F., Arístegui, J., Gasol, J. M., Lekunberri, I., & Herndl, G. J.: Mesoscale eddies: Hotspots of prokaryotic activity and differential community structure in the ocean. *ISME J.*, 4, 975–988, <https://doi.org/10.1038/ismej.2010.33>, 2010.

Belkin, N., Guy-haim, T., Rubin-blum, M., Lazar, A., and Sisma-, G.: Influence of cyclonic and anti-cyclonic eddies on plankton biomass , activity and diversity in the southeastern Mediterranean Sea. *Ocean Sci.*, 18, 693–715, <https://doi.org/10.5194/os-18-693-2022>, 1–56, 2022.

Benner, R., and Amon, R. M. W.: The size-reactivity continuum of major bioelements in the ocean. *Annu. Rev. Mar. Sci.* 7, 185–205. doi: 10.1146/annurev-marine-010213-135126, (2015).

Borchard, C. and Engel, A.: Organic matter exudation by *Emiliana huxleyi* under simulated future ocean conditions, *Biogeosciences*, 9, 3405–3423, doi:10.5194/bg-9-3405-2012, 2012

~~Carlson, C. A.: Baña, Z., Abad, N., Uranga, A., Azúa, I., Artolozaga, I., Unanue, M., Iriberry, J., Arrieta, J. M., and Ayo, B.: Recurrent seasonal changes in bacterial growth efficiency, metabolism and community composition in coastal watersProduction and Removal Processes. Chapter 4 in Biogeochemistry of Marine Dissolved Organic Matter, Editor(s): Hansell D. A., Carlson, C. A. AP, 805, 91–151. <https://doi.org/10.1016/b978-012323841-2/50006-3>. 2002.~~

Chelton, D. B., Gaube, P., Schlax, M. G., Early, J. J., and Samelson, R. M.: The Influence of Nonlinear Mesoscale Eddies on Near-Surface Oceanic Chlorophyll. *Science* 334, 328–333, 2011.

~~*Environ. Microbiol.*, 22, 369–380, <https://doi.org/10.1111/1462-2920.14853>. 2020.~~

~~Baña, Z., Ayo, B., Marrasé, C., Gasol, J. M., and Iriberry, J.: Changes in bacterial metabolism as a response to dissolved organic matter modification during protozoan~~

grazing in coastal Cantabrian and Mediterranean waters, *Environ. Microbiol.*, 16, 498–511, <https://doi.org/10.1111/1462-2920.12274>, 2014.

Bergkvist, J., Klawonn, I., Whitehouse, M. J., Lavik, G., Brüchert, V., & Ploug, H.: Turbulence simultaneously stimulates small and large scale CO₂ sequestration by chain-forming diatoms in the sea. *Nat. Commun.*, 9, 1–10, <https://doi.org/10.1038/s41467-018-05149-w>, 2018.

Bergstedt, M. S., Hondzo, M. M., and Cotner, J. B.: Effects of small scale fluid motion on bacterial growth and respiration, *Freshw. Biol.*, 49, 28–40, <https://doi.org/10.1046/j.1365-2426.2003.01162.x>, 2004.

Briand, E., Pringault, O., Jacquet, S., and Torr  ton, J. P.: The use of oxygen microprobes to measure bacterial respiration for determining bacterioplankton growth efficiency. *Limnol. Oceanogr. Meth.*, 2, 406–416, <https://doi.org/10.4319/lom.2004.2.406>, 2004.

Busch, K., Endres, S., Iversen, M. H., Michels, J., N  thig, E. M., and Engel, A.: Bacterial colonization and vertical distribution of marine gel particles (TEP and CSP) in the arctic Fram Strait, *Front. Mar. Sci.*, 4, 1–9. <https://doi.org/10.3389/fmars.2017.00166>, 2017.

Carr, M. E.: Estimation of potential productivity in Eastern Boundary Currents using remote sensing, *Deep-Sea Res. II: Top. Stud. Oceanogr.*, 49, 59–80, [https://doi.org/10.1016/S0967-0645\(01\)00094-7](https://doi.org/10.1016/S0967-0645(01)00094-7), 2001.

Cheney, R. E., and Richardson, P. L.: Observed Decay of a Cyclonic Gulf Stream Ring, *Deep-Sea Res. Oceanogr. Abstr.*, 23, 143–155, [https://doi.org/10.1016/S0011-7471\(76\)80023-X](https://doi.org/10.1016/S0011-7471(76)80023-X), 1976.

Cherrier, J., Valentine, S. K., Hamill, B., Jeffrey, W. H., and Marra, J. F.: Light-mediated release of dissolved organic carbon by phytoplankton. *J. Mar. Syst.*, 147: 45–51, 2015.

Christaki, U., Gueneugues, A., Liu, Y., Blain, S., Catala, P., Colombet, J., Debeljak, P., Jardillier, L., Irion, S., Planchon, F., Sassenhagen, I., Sime-Ngando, T., & Obernosterer, I.: Seasonal microbial food web dynamics in contrasting Southern Ocean productivity regimes. *Limnol. Oceanogr.*, 66(1), 108–122, <https://doi.org/10.1002/lno.11591>, 2021.

Couespel, D., L  vy, M., & Bopp, L.: Oceanic primary production decline halved in eddy-resolving simulations of global warming, *Biogeosciences*, 18(14), 4321–4349, <https://doi.org/10.5194/bg-18-4321-2021>, <https://doi.org/10.5194/bg-18-4321-2021>, 2021.

D'Asaro, E. A.: Generation of submesoscale vortices: A new mechanism, *J. Geophys. Res.*, 93, 6685-6693, <https://doi.org/10.1029/JC093iC06p06685>, <https://doi.org/10.1029/JC093iC06p06685>, 1988.

del Giorgio, P. A., and Cole, J. J.: Bacterial Growth Efficiency in Natural Aquatic Systems. *Annu. Rev. Ecol. Evol. Syst.*, 29, 503-541, <https://doi.org/10.1146/annurev.ecolsys.29.1.503>, 1998.

Del Giorgio, P. A., Condon, R., Bouvier, T., Longnecker, K., Bouvier, C., Sherr, E., and Gasol, J. M.: Coherent patterns in bacterial growth, growth efficiency, and leucine metabolism along a northeastern Pacific inshore – offshore transect. *Limnol. Oceanogr.*, 56(1), 1–16, <https://doi.org/10.4319/lo.2011.56.1.0001>, 2011.

Demarcq, H. and Somoue, L.: Phytoplankton and primary productivity off Northwest Africa. In: *Oceanographic and biological features in the Canary Current Large Marine Ecosystem*. Valdés, L. and Déniz-González, I. (eds). IOC-UNESCO, Paris. IOC Technical Series, No. 115, pp. 161-174. URI: <http://hdl.handle.net/1834/9186>. 2015.

Descy, J. P., Leporcq, B., Viroux, L., François, C., ~~&and~~ Servais, P.: Phytoplankton production, exudation and bacterial reassimilation in the River Meuse (Belgium). *J. Plankton Res.*, 24(3), 161-166. <https://doi.org/10.1093/plankt/24.3.161>, 2002.

Dickson, A. G., Sabine, C. L., and Christian, J. R.: *Guide to Best Practices for Ocean CO₂ measurements*. -PICES Special Publication 3, 191 pp., 2007.

Dittmar, T., Cherrier, J., and Ludwichowski, K. U.: The analysis of amino acids in seawater, in: *Practical guidelines for the analysis of seawater*, ed. by Oliver Wurl Boca Raton [u.a.], CRC Press, ISBN: 978-1-4200-7306-5, 2009.

Dray, S.: On the number of principal components: A test of dimensionality based on measurements of similarity between matrices, *Comput. Stat. Data Anal.*, 52, 4, 2228-2237, 2008.

~~Eichinger, M., Sempéré, R., Grégori, G., Charrière, B., Poggiale, J. C., and Lefèvre, D.: Increased bacterial growth efficiency with environmental variability: Results from DOC degradation by bacteria in pure culture experiments, *Biogeosciences*, 7(6), 1861-1876, <https://doi.org/10.5194/bg-7-1861-2010>, 2010.~~

Engel, A., and Galgani, L.: ~~The organic sea-surface microlayer in the upwelling region off the Coast of Peru and potential implications for air-sea-exchange processes. Biogeosciences, 13(4), 989–1007, <https://doi.org/10.5194/bg-13-989-2016>, 2016.~~

~~Engel, A., Goldthwait, S., Passow, U., and Alldredge, A.: Temporal decoupling of carbon and nitrogen dynamics in a mesocosm diatom bloom~~Engel, A., Borchard, C., Piontek, J., Schulz, K. G., Riebesell, U., and Bellerby, R.: CO₂ increases ¹⁴C primary production in an Arctic plankton community. Biogeosciences, 10(3), 1291–1308. <https://doi.org/10.5194/bg-10-1291-2013>, 2013.

~~Limnol. Oceanogr. 47, 753–761, doi: 10.4319/lo.2002.47.3.0753, 2002.~~

Engel, A., Händel, N., Wohlers, J., Lunau, M., Grossart, H. P., Sommer, U., and Riebesell, U.: Effects of sea surface warming on the production and composition of dissolved organic matter during phytoplankton blooms: Results from a mesocosm study, J. Plankton Res., 33(3), 357–372, <https://doi.org/10.1093/plankt/fbq122>, 2011.

Engel, A., Thoms, S., Riebesell, U., Rochelle-Newall, E., and Zondervan, I.: Polysaccharide aggregation as a potential sink of marine dissolved organic carbon. Nature, 428(6986), 929–932. <https://doi.org/10.1038/nature02453>, 2004.

Evans, C. A., O'Reily, J. E., and Thomas, J. P.: A handbook for measurement of Chl a and primary production, College Station, TX: Texas A & M University, 1987.

Ewart, C. S., Meyers, M. K., Wallner, E. R., McGillicuddy, D. J., and Carlson, C. A.: Microbial dynamics in cyclonic and anticyclonic mode-water eddies in the northwestern Sargasso Sea, Deep-Sea Res. II: Top. Stud. Oceanogr., 55(10–13), 1334–1347. <https://doi.org/10.1016/j.dsr2.2008.02.013>, 2008.

Falkowski, P. G., Ziemann, D., Kolber, Z., and Bienfang P. K.: Role of eddy pumping in enhancing primary production in the ocean, Letters to Nature, Vol 352, 1991.

Feng, M., Majewski, L. J., Fandry, C. B., and Waite, A. M.: Characteristics of two counter-rotating eddies in the Leeuwin Current system off the Western Australian coast, Deep-Sea Res. II: Top. Stud. Oceanogr., 54(8–10), 961–980, <https://doi.org/10.1016/j.dsr2.2006.11.022>, 2007.

~~Fischer, T., Karstensen, J., Dengler, M., and Bendinger, A.: Multiplatform observation of cyclonic eddies during the REEBUS experiment, EGU General Assembly 2021, online, 19–30 Apr 2021, EGU21-6537, <https://doi.org/10.5194/egusphere-egu21-6537>, 2021.~~

Gargas, E.: A Manual for Phytoplankton Primary Production Studies in the Baltic, The Baltic Marine Biologists, 2, 88 p., 1975.

Gasol, J.M., del Giorgio, P.A.: Using flow cytometry for counting natural planktonic bacteria and understanding the structure of planktonic bacterial communities. Sci. Mar. 64, 197–224. 2000.

Gattuso J. P., Epitalon J. M., Lavigne H. and Orr J.,: seacarb: seawater carbonate chemistry, R package version 3.2.13, <http://CRAN.R-project.org/package=seacarb>, 2020.

~~Gruber, N., Lachkar, Z., Frenzel, Grasshoff K., Kremling K., Ehrhardt M. : Methods of seawater analysis. Wiley-VCH, Weinheim, 1999.~~

~~H., Marchesiello, P., Münnich, M., McWilliams, J. C., Nagai, T., and Plattner, G. K.: Eddy-induced reduction of biological production in eastern boundary upwelling systems. Nat. Geosci., 4(11), 787–792, <https://doi.org/10.1038/ngeo1273>, 2011.~~

~~Guillemette, F., Leigh McCallister, S. and del Giorgio, P.: Selective consumption and metabolic allocation of terrestrial and algal carbon determine allochthony in lake bacteria, ISME J., 10, 1373–1382, <https://doi.org/10.1038/ismej.2015.215>, 2016.~~

Hansell, D. A., Carlson, C. A., Repeta, D. J., ~~&and~~ Schlitzer, R.: Dissolved organic matter in the ocean a controversy stimulates new insights. Oceanogr., 22(SPL.ISS. 4), 202–211. <https://doi.org/10.5670/oceanog.2009.109>, -2009.

Hernández-Hernández, N., Arístegui, J., Montero, M. F., Velasco-Senovilla, E., Baltar, F., Marrero-Díaz, Á., Martínez-Marrero, A., and Rodríguez-Santana, Á.: Drivers of Plankton Distribution Across Mesoscale Eddies at Submesoscale Range, Front.-Mar.-Sci., 7, 1-13. <https://doi.org/10.3389/fmars.2020.00667>, 2020.

Ihaka R., and Gentleman R.: R: a language for data analysis and graphics. J. Comput. Graph. Stat. 5, 299, 1996

Jiao, N., Robinson, C., Azam, F., Thomas, H., Baltar, F., Dang, H., Hardman-Mountford, N. J., Johnson, M., Kirchman, D. L., Koch, B. P., Legendre, L., Li, C., Liu, J., Luo, T., Luo, Y. W., Mitra, A., Romanou, A., Tang, K., Wang, X., Zhang, R. Mechanisms of microbial

carbon sequestration in the ocean - Future research directions. Biogeosciences, 11(19), 5285–5306. <https://doi.org/10.5194/bg-11-5285-2014>. 2014.

Karstensen, J., Fiedler, B., Schütte, F., Brandt, P., Körtzinger, A., Fischer, G., Zantopp, R., Hahn, J., Visbeck, M., and Wallace, D.: Open ocean dead zones in the tropical North Atlantic Ocean, *Biogeosciences*, 12, 2597-2605, <https://doi.org/10.5194/bg-12-2597-2015>, 2015.

Kelley, D. E.: Oceanographic Analysis with R. Oceanographic Analysis with R. <https://doi.org/10.1007/978-1-4939-8844-0>, 2018.

Kim, B., Kim, S. H., Kwak, J. H., Kang, C. K., Lee, S. H., & Hyun, J. H.: Heterotrophic bacterial production, respiration, and growth efficiency associated with upwelling intensity in the Ulleung Basin, East Sea. *Deep Sea Res. Part II Top. Stud. Oceanogr.*, 143, 24-35, <https://doi.org/10.1016/j.dsr2.2017.07.002>, <https://doi.org/10.1016/j.dsr2.2017.07.002>, 2017.

Kirchman, D., K'nees, E., and Hodson, R.: Leucine incorporation and its potential as a measure of protein synthesis by bacteria in natural aquatic systems, *Appl. Environ. Microbiol.*, 49(3), 599-607, <https://doi.org/10.1128/aem.49.3.599-607.1985>, 1985.

Lasternas, S., and Agustí, S.: The percentage of living bacterial cells related to organic carbon release from senescent oceanic phytoplankton, *Biogeosciences*, 11, 6377-6387, <https://doi.org/10.5194/bg-11-6377-2014>, 2014.

Lasternas, S., Piedeleu, M., Sangrà, P., Duarte, C. M., and Agustí, S.: Forcing of dissolved organic carbon release by phytoplankton by anticyclonic mesoscale eddies in the subtropical NE Atlantic Ocean. *Biogeosciences*, 10(3), 2129-2143, <https://doi.org/10.5194/bg-10-2129-2013>, 2013.

Lathuilière, C., Echevin, V., and Lévy, M.: Seasonal and intraseasonal surface Chl a-a variability along the northwest African Coast, *J. Geophys. Res.-Oceans*, 113, C05007. <https://doi.org/10.1029/2007JC004433>, 2008.

Le Vu, B., Stegner, A., Arsouze, T.: Angular momentum eddy detection and tracking algorithm (AMEDA) and its application to coastal eddy formation, *J. Atmos. Oceanic Technol.* 35, 739-762. <https://doi.org/10.1175/JTECH-D-17-0010.1>, 2018.

~~Lee, M. M., and Williams, R. G.: The role of eddies in the isopycnic transfer of nutrients and their impact on biological production, J. Levitus, S.: Climatological atlas of the World Ocean. NOAA Prof. Pap. 13, 1–41, 1982.~~

~~J. Mar. Res., 58(6), 895–917, <https://doi.org/10.1357/002224000763485746>, 2000.~~

Lévy, M., Klein, P., and Treguier, A. M.: Impact of submesoscale physics on production and subduction of phytoplankton in an oligotrophic regime, J. Mar. Res., 59(4), 535–565, 2001.

Lindroth P., Mopper K.: High performance liquid chromatographic determination of subpicomole amounts of amino acids by precolumn fluorescence derivatization with o-phthaldialdehyde, Anal. Chem., 51, 1667–1674, <https://doi.org/10.1021/ac50047a019>, 1979.

Lipson, D. A.: The complex relationship between microbial growth rate and yield and its implications for ecosystem processes. Front. Microbiol., 1–5. <https://doi.org/10.3389/fmicb.2015.00615>. 2015.

Lochte, K., and Pfannkuche, O.: Cyclonic cold-core eddy in the eastern North Atlantic. II. Nutrients, phytoplankton and bacterioplankton, Mar. Ecol. Prog. Ser., 39, 153–164. <https://doi.org/10.3354/meps039153>, 1987.

Lønborg, C., Martínez-García, S., Teira, E., and Álvarez-Salgado, X. A.: Bacterial carbon demand and growth efficiency in a coastal upwelling system. Aquat. Microb. Ecol., 63(2), 183–191. <https://doi.org/10.3354/ame01495>, 2011.

López-Urrutia, Á., and Morán, X. A. G.: Resource limitation of bacterial production distorts the temperature dependence of oceanic carbon cycling, Ecology, 88(4), 817–822, <https://doi.org/10.1890/06-1641>, 2007.

Löscher, C. R., Fischer, M. A., Neulinger, S. C., Fiedler, B., Philippi, M., Schütte, F., Singh, A., Hauss, H., Karstensen, J., Körtzinger, A., Künzel, S., and Schmitz, R. A.: Hidden biosphere in an oxygen-deficient Atlantic open-ocean eddy: Future implications of ocean deoxygenation on primary production in the eastern tropical North Atlantic, Biogeosciences, 12, 7467–7482, <https://doi.org/10.5194/bg-12-7467-2015>, 2015.

Lovecchio, E., Gruber, N., ~~&~~ Münnich, M.: Mesoscale contribution to the long-range offshore transport of organic carbon from the Canary Upwelling System to the open North

1214 Atlantic. Biogeosciences, 15(16), 5061–5091. <https://doi.org/10.5194/bg-15-5061-2018>,
1215 2018.

1216 Lovecchio, E., Gruber, N., Münnich, M., and Lachkar, Z.: On the long-range offshore
1217 transport of organic carbon from the Canary Upwelling System to the open North Atlantic,
1218 Biogeosciences, 14(13), <https://doi.org/10.5194/bg-14-3337-2017>, 2017.

1219 Mahadevan, A.: The Impact of Submesoscale Physics on Primary Productivity of Plankton,
1220 Annu. Rev. Mar. Sci., 8, 161-184, <https://doi.org/10.1146/annurev-marine-010814-015912>,
1221 2016.

1222 Maixandeau, A., Lefevre, D., Karayanni, H., Christaki, U., VanWambeke, F., Thyssen, M.,
1223 Denis, M., Fernandez, C.I., Uitz, J., Leblanc, K., Queguiner, B.: Microbial community
1224 production, respiration, and structure of the microbial food web of an ecosystem in the
1225 northeastern Atlantic Ocean, J. Geophys. Res. Oceans, 110 (C7), C07S17, 2005.

1226 ~~Marañón E, Cermeño P, Fernández E, Rodríguez J, Zabala L.: Significance and mechanisms~~
1227 ~~of photosynthetic production of dissolved organic carbon in a coastal eutrophic ecosystem,~~
1228 ~~Limnol Oceanogr, 49, 1652–1666, 2004.~~

1229 ~~Marbá, N., Duarte, C. M., and Agustí, S.: Allometric scaling of plant mortality rate, P. Natl.~~
1230 ~~Aead. Maßmig, M., Lüdke, J., Krahmann, G., and Engel, A.: Bacterial degradation activity~~
1231 ~~in the eastern tropical South Pacific oxygen minimum zone. Biogeosciences, 17(1), 215–~~
1232 ~~230. <https://doi.org/10.5194/bg-17-215-2020>, 2020.~~

1233 ~~Sci. USA, 104, 15777–15780, 2007.~~

1234 McGillicuddy Jr, D. J., Anderson, L. A., Doney S. C., and Maltrud, M. E.: Eddy-driven
1235 sources and sinks of nutrients in the upper ocean-: Results from a 0 . 1 ° resolution model
1236 of the North Atlantic, Glob. Biogeochem. Cycles., 17(2), 1035,
1237 <https://doi.org/10.1029/2002GB001987>, 2003.

1238 ~~McGillicuddy, D. J., and Robinson, A. R.: Eddy induced nutrient supply and new~~
1239 ~~production in the Sargasso Sea, Deep-Sea Res. I: Oceanogr. Res. Pap., 44(8), 1427-1450,~~
1240 ~~[https://doi.org/10.1016/S0967-0637\(97\)00024-1](https://doi.org/10.1016/S0967-0637(97)00024-1), 1997.~~

1241 McGillicuddy, D. J.: Mechanisms of Physical-Biological-Biogeochemical Interaction at the
1242 Oceanic Mesoscale, In Annual Review of Marine Science (Vol. 8),
1243 <https://doi.org/10.1146/annurev-marine-010814-015606>, 2016.

- ~~Mied, R. P., J. C. McWilliams, and Lindemann G. J.: The generation and evolution of mushroom-like vortices, J. Phys. Oceanogr., 21, 489–510, 1991.~~
- Molemaker, M. J., McWilliams, J. C., and Dewar, W. K.: Submesoscale generation of mesoscale anticyclones near a separation of the California Undercurrent, J. Phys. Oceanogr., 45, 613–629, <https://doi.org/10.1175/JPO-D-13-0225.1>, 2015.
- Mouriño-Carballido, B., and McGillicuddy, D. J.: Mesoscale variability in the metabolic balance of the Sargasso Sea, Limnol. Oceanogr., 51(6), 2675–2689, <https://doi.org/10.4319/lo.2006.51.6.2675>, 2006.
- Mouriño-Carballido, B.: Eddy-driven pulses of respiration in the Sargasso Sea, Deep-Sea Res. I: Oceanogr. Res. Pap., 56(8), 1242–1250, <https://doi.org/10.1016/j.dsr.2009.03.001>, 2009.
- Mühlenbruch, M., Grossart, H. P., Eigemann, F., and Voss, M.: Mini-review: Phytoplankton-derived polysaccharides in the marine environment and their interactions with heterotrophic bacteria. Environ. Microbiol., 20(8), 2671–2685. <https://doi.org/10.1111/1462-2920.14302>, 2018.
- Neijssel, O. M., and Mattos, M. J. T. De.: Micro Review The energetics of bacterial growth : a reassessment, 13(2), 179–182, 1994.
- Nielsen, E. S.: The use of radio-active carbon (c14) for measuring organic production in the sea, ICES Mar. Sci., 18(2), 117–140, <https://doi.org/10.1093/icesjms/18.2.117>, 1952.
- Noyon, M., Morris, T., Walker, D., ~~&and~~ Huggett, J.: Plankton distribution within a young cyclonic eddy off south-western Madagascar, Deep Sea Res. Part II Top. Stud. Oceanogr., 166, 141–150, <https://doi.org/10.1016/j.dsr2.2018.11.001>, ~~2018~~2019.
- Obernosterer, I., and Herndl, G. J.: Phytoplankton extracellular release and bacterial growth: Dependence on the inorganic N:P ratio. Mar. Ecol. Prog. Ser., 116, 247–258, <https://doi.org/10.3354/meps116247>, 1995.
- Pegliasco, C., Chaigneau, A., and Morrow, R.: Main eddy vertical structures observed in the four major Eastern Boundary Upwelling Systems. J. Geophys. Res. Oceans, 120(9), 6008–6033, <https://doi.org/10.1002/2015JC010950>, 2015.
- Pelegri, J. L. and Peña-Izquierdo, J.: Eastern boundary currents off North-West Africa. In: Oceanographic and biological features in the Canary Current Large Marine Ecosystem.

Valdés, L. and Déniz-González, I. (eds). IOC- UNESCO, Paris. IOC Technical Series, No. 115, pp. 81-92, URI: <http://hdl.handle.net/1834/9179>, 2015

~~Piontek, J., Endres, S., Passow, U.: Transparent exopolymer particles (TEP) in aquatic environments, Le Moigne, F. A. C., Schartau, M., and Engel, A.: Relevance of Nutrient-Limited Phytoplankton Production and Its Bacterial Remineralization for Carbon and Oxygen Fluxes in the Baltic Sea. Front. Mar. Sci., 6, 1–16, <https://doi.org/10.3389/fmars.2019.00581>, 2019.~~

~~Prog. Oceanogr., 55(3–4), 287–333, [https://doi.org/10.1016/S0079-6611\(02\)00138-6](https://doi.org/10.1016/S0079-6611(02)00138-6), 2002.~~

~~Pete, R., Davidson, K., Hart, M. C., Gutierrez, T., and Miller, A. E. J.: Diatom derived dissolved organic matter as a driver of bacterial productivity: The role of nutrient limitation, J. Exp. Mar. Biol. Ecol., 391(1–2), 20–26, <https://doi.org/10.1016/j.jembe.2010.06.002>, 2010.~~

Rao, D. N., Chopra, M., Rajula, G. R., Durgadevi, D. S. L., and Sarma, V. V. S. S.: Release of significant fraction of primary production as dissolved organic carbon in the Bay of Bengal, Deep Sea Res. Part I Oceanogr. Res., 168, 1–27, <https://doi.org/10.1016/j.dsr.2020.103445>, 2021.

Regaudie-De-Gioux, A., and Duarte, C. M.: Temperature dependence of planktonic metabolism in the ocean. Glob. Biogeochem. Cycles, 26(1), GB1015, <https://doi.org/10.1029/2010GB003907>, 2012.

Reinthal, T., Bakker, K., Manuels, R., van Ooijen, J., ~~&and~~ Herndl, G. J.: Erratum to Fully automated spectrophotometric approach to determine oxygen concentrations in seawater via continuous-flow analysis. Limnol. Oceanogr. Methods 5(1), 72–72. ~~<https://doi.org/10.4319/lom.2007.5.72>, 2007~~<https://doi.org/10.4319/lom.2007.5.72>, 2006.

Robinson C.: Heterotrophic bacterial respiration. In: Kirchman DL (ed) Microbial ecology of the oceans, Wiley-Liss, New York, NY., 2008.

Russell, J. B. and Cook, M. G.: Energetics of Bacterial Growth : Balance of Anabolic and Catabolic Reactions, Microbiol Rev., 59(1), 48–62, 1995.

~~Schartau, M., Engel, A., Schröter, J., Thoms, S., Völker, C., and Wolf-Gladrow, D.: Modelling carbon overconsumption and the formation of extracellular particulate organic carbon, Biogeosciences, 4, 433-454, 2007.~~

Schlitzer, R.: Ocean Data View, odv.awi.de, 2020.

Schütte, F., Brandt, P., and Karstensen, J.: Occurrence and characteristics of mesoscale eddies in the tropical northeastern Atlantic Ocean, Ocean Sci., 12, 663-685, <https://doi.org/10.5194/os-12-663-2016>, 2016.

~~Seymour, J. R., Amin, S. A., Raina, J. B., and Stocker, R.: Zooming in on the phycosphere: The ecological interface for phytoplankton-bacteria relationships. Nat. Microbiol., 2, 17065, <https://doi.org/10.1038/nmicrobiol.2017.65>, 2017.~~

Simon, M., and Azam, F.: Protein content and protein synthesis rates of planktonic marine bacteria, Mar. Ecol. Prog. Ser., 51, 201-213, 1989.

Singh, A., Gandhi, N., Ramesh, R., & Prakash, S.: Role of cyclonic eddy in enhancing primary and new production in the Bay of Bengal, J. Sea Res, 97, 5-13, <https://doi.org/10.1016/j.seares.2014.12.002>, 2015.

Smith, D., and Azam, F.: A simple, economical method for measuring bacterial protein synthesis rates in seawater using. Mar. Microb. Food Webs, 6(2), 107-114, 1992.

~~Solorzano~~Solórzano, L.: Determination of Ammonia in Natural Waters by the Phenolhypochlorite Method, Limnol. Oceanogr., 14, 799-801, 1969.

Strickland, J.D.H. and Parsons, T.R.: A Practical Handbook of Seawater Analysis. Bulletin of Fisheries Research Board of Canada, 167, 1-311, 1968.

Thomsen, S.: The formation of a subsurface anticyclonic eddy in the Peru-Chile Undercurrent and its impact on the near-coastal salinity, oxygen, and nutrient distributions, J. Geophys. Res. Oceans, 121, 476-501, <https://doi.org/10.1002/2015JC010878>, 2016.

~~Thornton, D. C. O.: Dissolved organic matter (DOM) release by phytoplankton in the contemporary and future ocean, Eur. J. Phycol., 49(1), 20-46, <https://doi.org/10.1080/09670262.2013.875596>, 2014.~~

Vaqué, D., Alonso-Sáez, L., Arístegui, J., Agustí, S., Duarte, C. M., Montserrat Sala, M., Vázquez-Domínguez, E., and Gasol, J. M.: Bacterial production and losses to predators

1331 along an Open ocean productivity gradient in the Subtropical North East Atlantic Ocean. J.
1332 Plankton Res., 36(1), 198-213, <https://doi.org/10.1093/plankt/fbt085>, 2014.

1333 Wear, E. K., Carlson, C. A., and Church, M. J.: Bacterioplankton metabolism of
1334 phytoplankton lysates across a cyclone-anticyclone eddy dipole impacts the cycling of
1335 semi-labile organic matter in the photic zone, Limnol. Oceanogr., 65(7), 1608-1622,
1336 <https://doi.org/10.1002/lno.11409>, 2020.

1337 Wickham H.: tidyverse: Easily Install and Load ‘Tidyverse’ Packages. See [https://cran.r-](https://cran.r-project.org/package=tidyverse)
1338 [project.org/package=tidyverse](https://cran.r-project.org/package=tidyverse), 2016.

1339 Wilhelm, W. L.: Die Bestimmung des im Wasser gelösten Sauer- stoffes, Ber. Dtsch. Chem.
1340 Ges., 21, 2843-2854, 1888.

1341 ~~Wood, A. M., and van Valen, L. M.: Paradox lost? On the release of energy-rich compounds~~
1342 ~~by phytoplankton, Mar. Microb. Food Webs, 4, 103-116, 1990.~~

1343 Xu, G., Dong, C., Liu, Y., Gaube, P., and Yang, J.: Chl a Rings around Ocean Eddies in the
1344 North Pacific, Sci. Rep., 9(1), 1-8, <https://doi.org/10.1038/s41598-018-38457-8>, 2019.

1345 ~~Xu, J., Jing, H., Sun, M., Harrison, P. J., and Liu, H.: Regulation of bacterial metabolic~~
1346 ~~activity by dissolved organic carbon and viruses, J. Geophys. Res. Biogeosci., 118(4), 1573-~~
1347 ~~1583, <https://doi.org/10.1002/2013JG002296>, 2013.~~

1348 ~~Yan, W., Zhang, R., and Jiao, N.: A longstanding complex tropical dipole shapes marine~~
1349 ~~microbial — biogeography, — Appl. — Environ. — Microbiol., — 84(18),~~
1350 ~~<https://doi.org/10.1128/AEM.00614-18>, 2018.~~

1351 ~~Zhang, Y., Jiao, N., Sun, Z., Hu, A., & Zheng, Q.: Phylogenetic diversity of bacterial~~
1352 ~~communities in South China Sea mesoscale cyclonic eddy perturbations, Res. Microbiol.,~~
1353 ~~162(3), 320-329, <https://doi.org/10.1016/j.resmic.2010.12.006>, 2011.~~